



BIG-MAP



D5.3 – Demonstrating the capacity to run coordinated multi-technique, multi-site and multi-scale experiments

VERSION

VERSION	DATE
1.1	31/08/2023

PROJECT INFORMATION

GRANT AGREEMENT NUMBER	957189
PROJECT FULL TITLE	Battery Interface Genome - Materials Acceleration Platform
PROJECT ACRONYM	BIG-MAP
START DATE OF THE PROJECT	1/9-2020
DURATION	3 years
CALL IDENTIFIER	H2020-LC-BAT-2020-3
PROJECT WEBSITE	big-map.eu

DELIVERABLE INFORMATION

WP NO.	5
WP LEADER	Sandrine Lyonard
CONTRIBUTING PARTNERS	ESRF, CEA, ILL and all WP5 partners + CIDETEC, FZJ (WP4 and 6) and EPFL (WP9)
NATURE	Demonstrator
AUTHORS	F. Cadiou, C. Herrera, D. Blanchard, G. Baraldi, C. Wölke, Q. Jacquet, S. Lyonard
CONTRIBUTORS	All WP5 partners with participation from WP4, 6 (CIDETEC G. Baraldi and FZJ C. Wölke and I. Cekic-Laskovic) and 9 (F. Liot)
CONTRACTUAL DEADLINE	31/08/2023
DELIVERY DATE TO EC	31/08/2023
DISSEMINATION LEVEL (PU/CO)	PU

ACKNOWLEDGMENT



This project has received funding from the European Union's Horizon 2020 research and innovation programme under grant agreement No 957189. The project is part of BATTERY 2030+, the large-scale European research initiative for inventing the sustainable batteries of the future.



ABSTRACT

One of the principal aims of the BIG-MAP project is to establish a European characterisation platform for material science and accelerated material discovery related to battery applications. Towards this goal, and in parallel with the development of automatized tasks (material synthesis, experiments, and simulations) fostered by machine learning algorithms, an important contribution to the overall project success and a keystone of WP5 is employing advanced characterisation techniques to provide high-fidelity data. Due to their inherent complexity (e.g., experimental set-ups and data analysis), these techniques often require non-negligible human expert intervention.

Thus, the main objective of this report is to demonstrate the feasibility of executing coordinated multi-technique, multi-site, and multi-scale experiments, highlighting this on a selected chemistry. To achieve this purpose, an experimental workflow involving all partners in WP5 was designed and executed. As its base, an advanced chemistry of specific interest to the project was defined in coordination with WP4 and WP6 (coating & electrolyte WPs). Thereafter, a range of strategies was investigated to address the question of ex-situ / operando experimental coherence and reproducibility. Data and know-how gained from previous Tiers of WP5 experiments were collated and served as inputs in the creation of the new workflow. As a result, pan-European in-lab and Large Scale Facility (LSF) characterisation experiments were performed, probing a large range of temporal and spatial domains with various degrees of data fidelity.

In addition, innovations developed in the project with respect to experimental electrochemical cell harmonisation and the bespoke deployment of automated data visualisation and pre-treatment processes are reported.

The present deliverable focuses on data acquisition, and although links will be made to scientific outputs resulting from D5.3 experiments/data pre-treatment, it is not the intention to provide a detailed description of data analysis in this report, as this aspect is the subject of the upcoming D5.4 deliverable which has been conceived to conjoin with D5.3.



TABLE OF CONTENTS

1	GENERAL OVERVIEW OF THE WORK DESCRIBED IN D5.3	4
2	EXPERIMENTAL WORKFLOW ORGANISATION IN WP5	6
2.1	HISTORY OF WORK ORGANISATION BEFORE THE D5.3 DEMONSTRATOR	6
2.1.1	FIRST ORGANISATION (SPONTANEOUS AND MATRIX, TIER 1 EXPERIMENTS)	6
2.1.2	INDIVIDUAL OR SHORT-RANGE COOPERATIVE WORKFLOWS	7
2.2	THEORETICAL VIEW OF GLOBAL LONG-RANGE WORKFLOWS	9
3	PRACTICAL WORKFLOW APPLICATION IN THE SCOPE OF D5.3	12
3.1	GLOBAL WORKFLOW OVERVIEW	12
3.1.1	MOTIVATIONS	12
3.1.2	SAMPLES	13
3.1.3	EXPERIMENTAL TECHNIQUES	13
3.2	WORKFLOW DETAILS	15
3.2.1	BATTERY CYCLING PROTOCOL AND SAMPLE PROVIDING	16
3.2.2	SAMPLE REPARTITION AND DELIVERY WITH DATA TRACKING	21
3.2.3	TIMELY ORCHESTRATION OF D5.3	25
3.2.4	ORGANISATIONAL POINTS TO DISCUSS	27
3.3	SCIENTIFIC OUTCOMES	27
3.4	ON THE USE OF THE BIG-MAP ARCHIVE AND BIG-MAP NOTEBOOK	31
3.5	ON-THE-FLY VISUALISATION AND PRE-PROCESSING OF EXPERIMENTAL DATA	35
3.5.1	ELECTROCHEMISTRY DATA	35
3.5.2	VISUALISING RAW DATA AT LSFs	35
3.6	EXPERIMENTAL OPERANDO OR IN-SITU CELL HARMONISATION IN WP5 / D5.3	39
4	CONCLUSION, OUTLOOKS, AND LINKS TO D5.4 AND DATA ANALYSIS	40
5	ANNEXES	42
5.1	GLOSSARY FOR EXPERIMENTAL TECHNIQUES	42
5.2	LITDI DESCRIPTION AND ASSOCIATED PUBLICATIONS	43
5.3	SURVEY FORM USED TO GATHER D5.3 EXPERIMENTAL RESULT OVERVIEW	44
5.4	ADDITIONAL PLOTS FOR THE D5.3 SCIENTIFIC OUTCOMES	45
5.5	ADDITIONAL INFORMATION ON THE BIG-MAP ARCHIVE USAGE	48



1 General overview of the work described in D5.3

Task 5.3 of work package 5 (WP5) is to provide the proof of concept of running coordinated multi-technique experiments to acquire multi-scale data on battery cells and demonstrating this goal by practical application to selected chemistry.

This document reports the actions and steps performed to establish the demonstrator, from the start of WP5 operations to the design and achievement of the selected experiments in D5.3, according to the Task 5.2 workflow.

Included here are:

- The history of the experimental organisations established in WP5 that led to the present deliverable (section 2);
- The description of the specific demonstrator workflow for D5.3 (sections 3.1 and 3.2);
- An analysis and discussion resulting from collecting and aggregating the scientific and experimental output from the D5.3 workflow (section 3.3).

Figure 1 provides a glossary of the graphical elements used in Figure 2, Figure 5 and Figure 12.

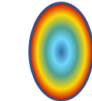
As an overview, Figure 2, articulated around three interconnected constituents, gives a graphical summary of the tasks performed in WP5 leading to D5.3 completion. Tier 1 experiments (left half part) refer to the initial period of the BIG-MAP project wherein WP5 commenced its first experimental activities as standards and protocols were defined and delivered by Work Package 8 (WP8) in parallel (discussed in section 2.1.1). The A insert (middle and bottom) is related to the ex-situ workflow designed to test reproducibility in sample preparation, shipment, and washing procedures (see details in section 2.1.2). Finally, block B (Tier 2 in the right half) represents the main focus of this document, *i.e.*, the D5.3 workflow demonstration (described in section 3).

Graphical glossary

Samples

-  Inhouse cell protocol and cycling
-  BIG-MAP cell assembly protocol and cycling
-  Unknown / not clearly defined negative and / or positive electrode
-  BIG-MAP provided negative electrode (Gr from CIDETEC)
-  BIG-MAP provided positive electrode (LNO from BASF)
-  BIG-MAP standard electrolyte (LP57 + VC)
-  BIG-MAP standardised advanced electrolyte (LP57 + VC + LiTDI)
-  Relative battery SoH before characterisation

Actions and reactions

-  Experiment
-  Paper and scientific dissemination
-  Correlation effort
-  Macro block detailed in a sub figure
-  Mutualisation and community effort
-  Difficulties / blocking points
-  Group / WP reaction and decision making

Tools - communication and organisation

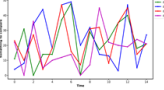
-  Scientific question on battery properties
-  Video conferencing
-  Local / in-person meetings
-  "Large scale" workshops / meetings gathering partners in-person
-  Close contact loops for "small scale" coordinated work
-  Online capabilities for storing and sharing data and metadata (online notebook and BIG-MAP archive)
-  Framework / workflow / organisation for sample preparation and sharing, experiment selection and preparation
-  Standard visualisation and data analysis tools (progress towards)

Figure 1. Graphical glossary for elements in Figure 2, Figure 5 and Figure 12

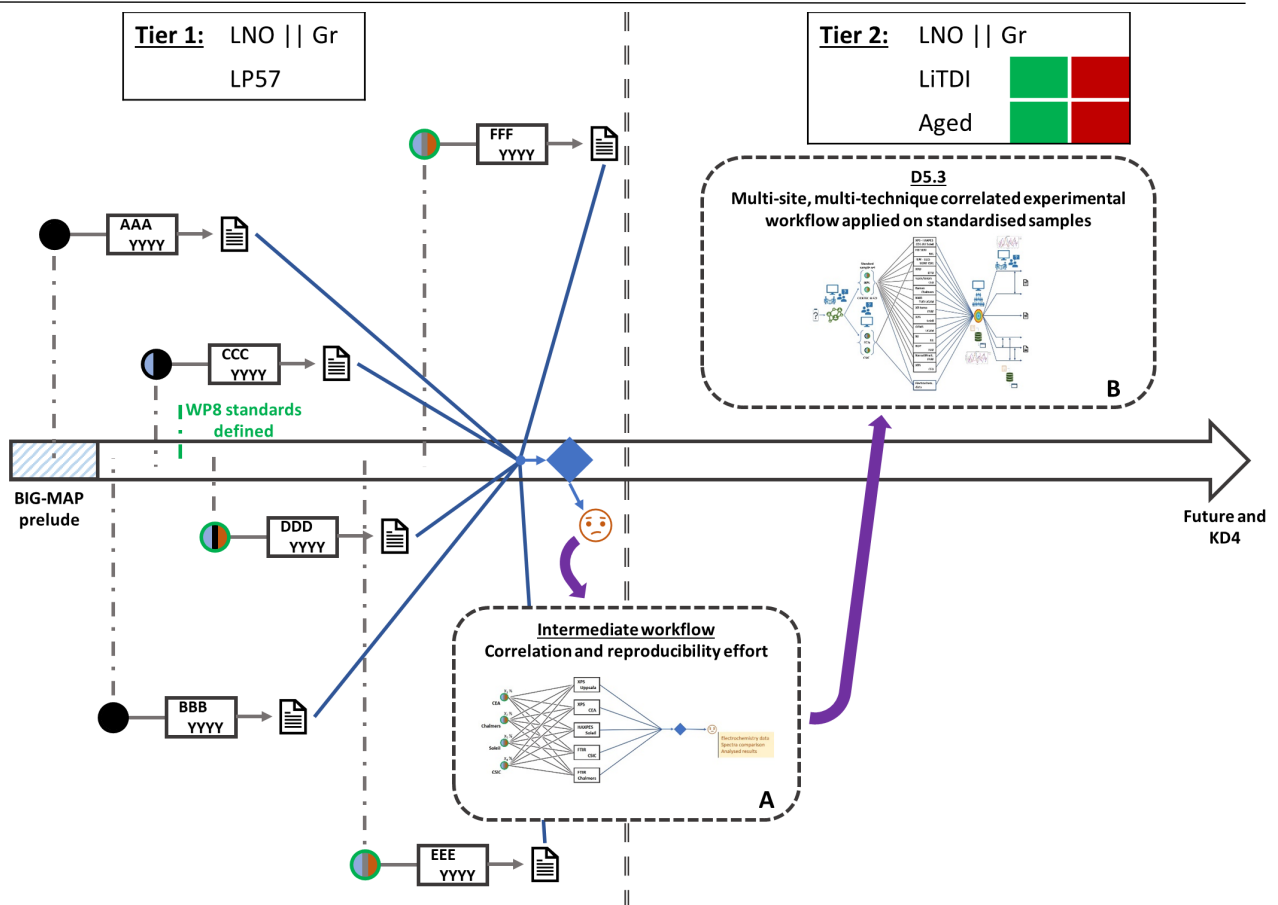


Figure 2. Main timeline for WP5 experimental work organisation leading to D5.3 and beyond

2 Experimental workflow organisation in WP5

The main objective of WP5 is to develop synergies to initiate a pilot for the implementation of a European multimodal experimental platform using standardised cells/protocols/metadata collection, data treatment, and post-analysis. WP5 gathers together multiple partners (15 partners, including two industrials, UMI and SAFT), each working in different fields and using a wide variety of complementary characterisation techniques. To ensure smooth and efficient workflows and to enable correlative use of the data generated from these multi-scale, multimodal characterisation experiments, detailed organisation, and planning is a *sine qua non* condition. The present section of this report describes the steps that led to the construction and execution of D5.3.

2.1 History of work organisation before the D5.3 demonstrator

To perform coordinated experiments and collaborative investigations in WP5, partners have tackled this problem by experimenting with different ways of working in unison to render the process more efficient. This subsection will address the subject from a conceptual and reporting point of view.

2.1.1 First organisation (spontaneous and matrix, Tier 1 experiments)

A survey to collect information on the different experimental techniques and cells available amongst all the partners in WP5 was carried out as a first step. This preliminary knowledge was then utilised to inform the different experimental possibilities within the work package. WP5, and more generally, all consortium partners could access this newly created catalogue for a complete



overview of the consortium's characterisation capabilities. The resulting experimental matrix provided the core of D5.1, the first deliverable within WP5.

Exploring the possibilities leveraged by this matrix led naturally to the adoption of an initial classical approach, designated as a “fully parallel workflow”, whereby each partner fabricates and characterises their samples using in-house expertise and techniques (Tier 1 experiments in Figure 2). Such a workflow, therefore, provides independent and often complementary datasets which theoretically can be summed/linked to obtain a more complete correlated analysis. This is illustrated in Figure 3.

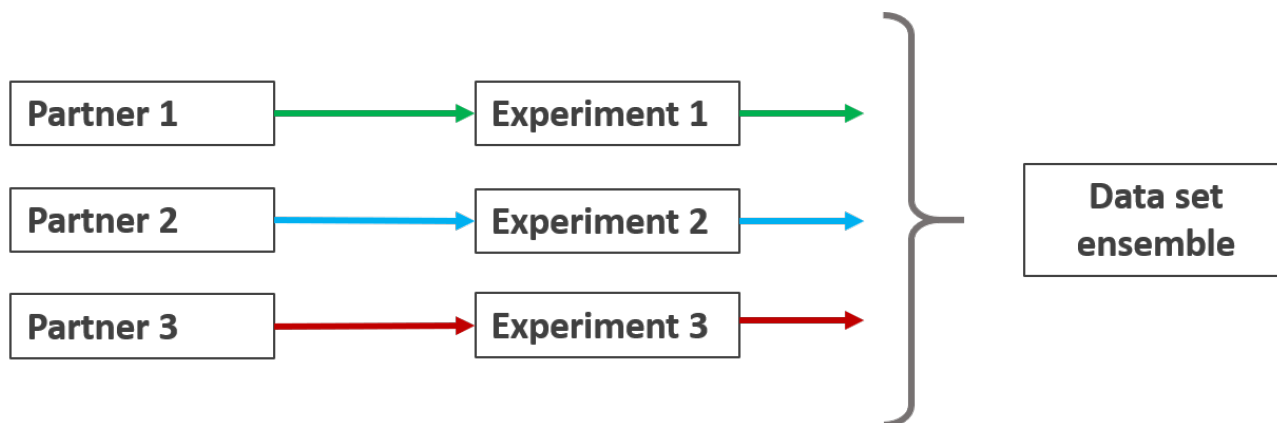


Figure 3. Schematic view of the first spontaneous fully parallel organisation in WP5

For this type of workflow, experiments do not require to be synchronised in time. Also, standardisation (cell material/assembly, cycling...) is minimal - indeed, some of the dataset associations were formed *a posteriori*. Moreover, a number of these Tier 1 experiments (*cf.* Figure 2) were also carried out prior to cell assembly and cycling protocols, as the BIG-MAP first standards and protocols were defined by WP8 in February 2021 (deliverables D8.1 and D8.3) and consequently updated in February 2022 with D8.4.

Hence, depending on the date, not all sample preparation followed these standard protocols. Also, in practice, some state-of-the-art high-fidelity techniques require specific sample size and/or preparation, notably for operando measurements, which do not necessarily conform with coin cell standards defined by WP8. Nevertheless, an effort was made by all partners to adapt as closely as possible their protocols to the BIG-MAP standards in these situations. This led to some difficulties and blocking points when correlating precisely the different experimental results. Therefore, the main identified blocking points were linked to the preliminary absence of clear standards and protocols. As an example, the different electrochemical data were not comparable because the electrodes varied in size, internal cell pressure, and amount of electrolyte and separator employed. Similarly, during cycling, the C-rate was not defined uniformly, and most of the time, when aging was involved, it was defined by the number of cycles and not the state of life, which is a more normalised metric. In such situations, the challenge of correlating results from differing experimental techniques was non-negligible as the probed objects are inherently different for each dataset. This difficulty is amplified when trying to establish correlations between results from diverse experimental domains.

2.1.2 Individual or short-range cooperative workflows

Following the first results and limitations encountered in the preliminary, spontaneous workflow, it became apparent that new and improved strategies were needed.



Firstly, a post-mortem surface spectroscopy workflow was initiated (A insert in Figure 2). This workflow aimed to investigate the possibility of preparing reproducible ex-situ samples in different WP5 labs. The reproducibility test was centered around surface spectroscopy measurements on samples prepared at different locations. Surface spectroscopy methods such as XPS were chosen because of their extreme sensitivity to sample preparation and handling. We opted to establish a post-mortem workflow, thereby enabling the elimination of the multitude of variables inherent to operando experiments which impact reproducibility. Several partners performed the tasks of assembling and then cycling their cells in line with standard protocols from WP8. These aged samples were then dispatched to several partners, all using similar surface spectroscopy techniques (e.g., FTIR, XPS), and this series of experimental results were centralised and compared (see Figure 4 for a conceptual graphical vision of the workflow).

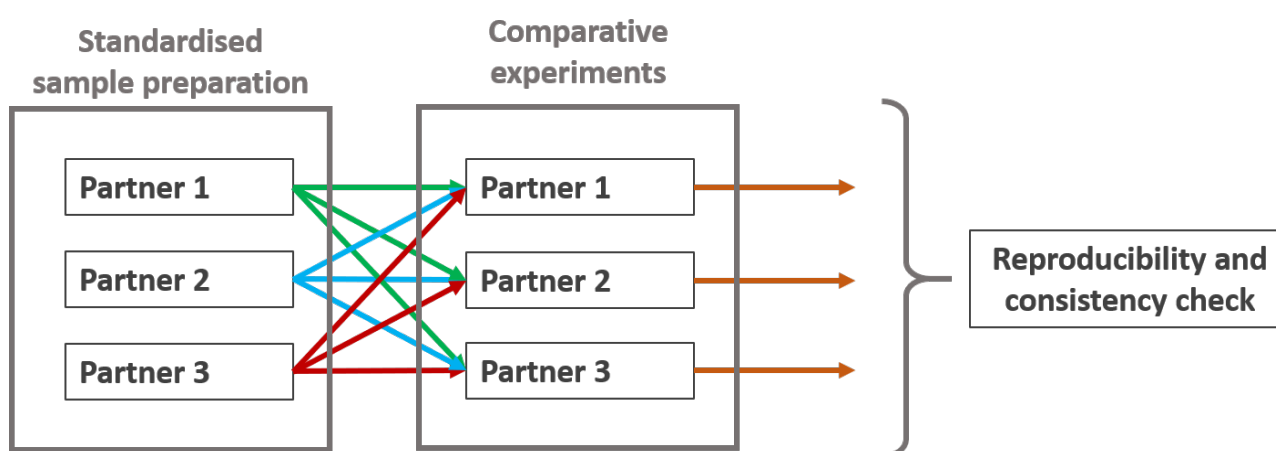


Figure 4. Reproducibility and consistency post-mortem workflow as a concept

Some details on the practical application of this workflow can be found in deliverable D5.5. To expand on this here, four partners (CEA, Chalmers, CSIC, and CNRS) were involved in the cell cycling. The samples were then dispatched for XPS analysis at CEA and UU, HAXPES at Soleil/CNRS, and FTIR at Chalmers and CSIC. This is illustrated in Figure 5.

In practice, sample preparation, cycling, shipping, and experiments were all carried out from September 2021 to April 2022. Nevertheless, although there was a notable improvement in the consistency of the sample state, notably due to all partners' adherence to assembly and cycling protocols outlined in WP8, achieving globally consistent electrochemical cell behaviour between different partners remained challenging. This inevitably led to difficulties comparing and correlatively analysing the different spectra obtained, particularly for XPS and HAXPES data.

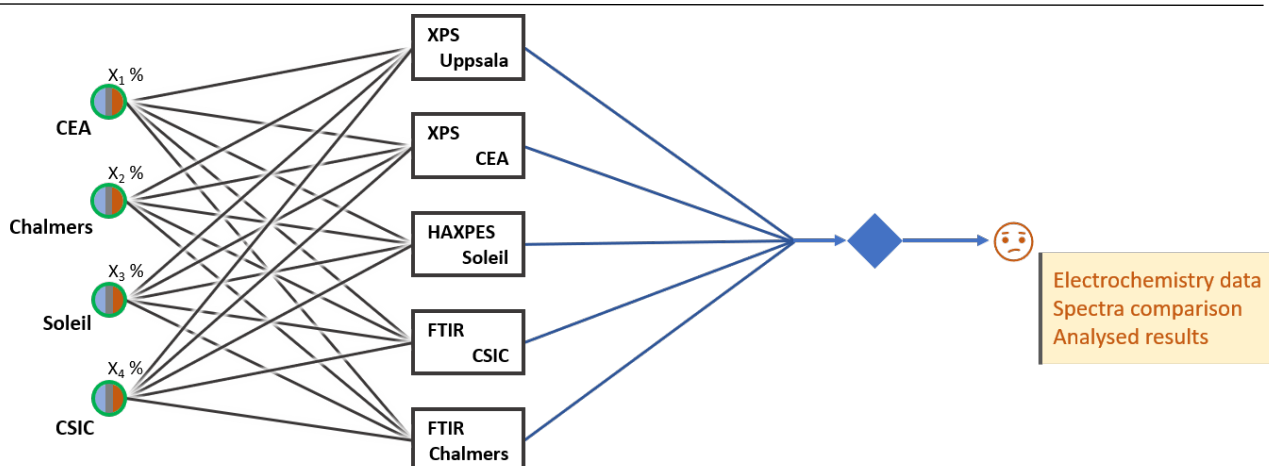


Figure 5. Intermediate key demonstrator focusing on surface spectroscopic measurements and reproducibility analysis. Black links symbolising a sample flux while the blue ones represent a data and metadata flux.

A second work axis taken was to theorise the use of short-range experimental workflows, as discussed in D5.5. In D5.5, WP5 focused on developing an organisational architecture for an automatable experimental workflow. This architecture was designed to align with the efforts made in WP8 regarding standardisation and the connections with WP9, 10, and 11 for achieving interoperability, automation, and the incorporation of Artificial Intelligence (AI) modules.

The D5.5 organisational framework was crafted with a focus on adaptability and evolutive decision-making, specifically targeting one or a few interconnected experimental techniques. To obtain optimal efficiency, the nature of this approach inherently restricted the number of participating partners involved in the correlative work, hence the name short-range experimental workflow. Further details about this framework are presented in deliverable D5.5.

However, we concluded that this framework might not be the most suitable choice for a broad-range experimental workflow, *i.e.*, a long-range workflow, as intended for in D5.3, which aimed at collaboration from all WP5 partners in their specific fields of expertise. Consequently, we opted to explore alternative approaches.

2.2 Theoretical view of global long-range workflows

We theorised different workflow patterns to build the D5.3 demonstrator architecture. These patterns illustrate four types of working organisations schematically represented in Figure 6, Figure 7, Figure 8 and Figure 9.

As mentioned, the primary limitation identified in previous workflows was that, despite adhering to the standards and protocols from WP8, the consistency in sample preparation was insufficient to establish a strong correlation between datasets within a multi-site, multi-technique framework. Hence, special attention must be paid to sample preparation when aiming for a correlative approach across such a diverse array of techniques, as encountered in WP5. The common denominator forming the basis of the consequent workflow designs was thus to start from the same standardised sample. In practice, this entails that the full workflow is performed on the same standard sample or several samples made as identical as possible through thorough standardisation procedures (preparation, cycling, rinsing...). Samples obtained from either of these approaches can then be cut and dispatched to several partners. As an example, using a single electrode from a cycled pouch or



coin cell, it is possible to use the same physical piece as a sample (eventually probing the same area) for each experiment in the workflow or to cut the original electrode into several parts to be sent to different partners. This method readily lends itself to parallel acquisitions and/or comparisons, hence optimising the timescale needed, but also for destructive experimental techniques and specific, bespoke sample preparation needed for certain experimental set-ups.

The first of these workflow patterns is another parallelised workflow (*cf.* Figure 6 in comparison with Figure 3 and Figure 4), where the initial sample is distributed to a set number of involved partners. Some of the experimental techniques performed by more than one partner can be identical in order to check for reproducibility and coherence if deemed necessary. Furthermore, this approach enables the synchronised execution of a wide-ranging set of experiments, as each selected experiment is allocated its own piece of the initial sample. Consequently, factors such as sample preparation and destructiveness do not significantly impact the process, provided there is an adequate supply of initial standard sample material to support each experiment (for instance, a sufficient number of coin cells or large enough pouch cells). This type of workflow can then generate correlated datasets covering a wide array of properties, from microstructure images to diffraction patterns and chemical or electronic bonding maps.

Moreover, one advantage of this approach is its simplicity and ease of set-up regarding time constraints. The unavoidable time considerations are only due to the duration required for standardised sample preparation, including delivery to the partners and meeting the final deadline to collect all the measured datasets. The downside of adopting such a highly diversified workflow pattern is the inability to establish a precise and rigorous spatial correlation between the datasets. This limitation arises because each dataset originates from a distinct physical part of the standard sample.

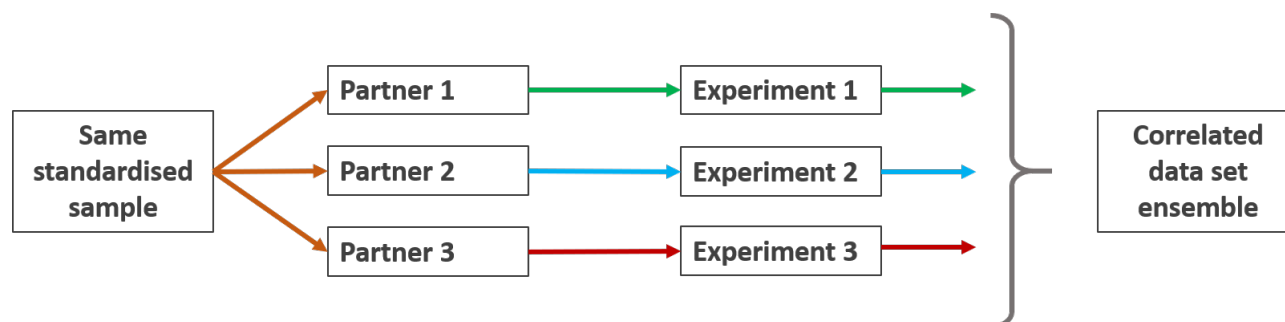


Figure 6. A new parallel standardised workflow

The counterpart of such a parallelised pattern is naturally a fully sequential one (*cf.* Figure 7), where all experiments are performed in a well-defined area of the very same physical piece of the electrode. With such a workflow, it is possible to obtain a full spatial correlation in the collected datasets. Such a correlation is simple to imagine for ex-situ samples as long as the sample is neither damaged nor altered from one experiment to another. Of course, this implies that only non-destructive experiments can be employed, with the exception of the very last test, to guarantee the exact spatial correlation. Inserting in-situ or operando steps into this experimental mix automatically raises questions concerning the correlation. Naturally, the spatial correlation remains valid, excluding, of course the case of destructive testing, but the temporal correlation is shifted by each in-situ / operando step as all experiments are sequential by design. Some facilities and machines can offer to use more than one technique simultaneously (like the instrument NeXT at ILL where



neutron and X-ray imaging can be performed simultaneously), which can solve some of the issues, but these are relatively rare. Depending on the elected timeframes for the experiments, this might not be a problem if the sample state remains unchanged or negligible changes occur over all experiments. However, this is not always true, for example, if one wants to look at SEI formation in Si containing electrodes. In this particular case, the very first formation cycle is very important, impeding spatial correlation from several consecutive operando measurements as the sample state would largely differ from one experiment to the next. Transferring samples across all techniques in the workflow can pose challenges, as it may not be straightforward due to certain technique-specific characteristics. Therefore, compatibility between the techniques must be carefully examined, considering factors such as sample format and preparation, the type of cell used, and sample holder requirements. Some information on experimental method compatibility is cited for WP5 in the experimental matrix in D5.1 and hints / thoughts on how to proceed have also been gathered in D5.5. From a purely logistical perspective, this organisation is most affected by the time required for various steps and the potential delays in sample transfer and delivery. As a result, it needs to be closely monitored and meticulously planned to ensure smooth execution.

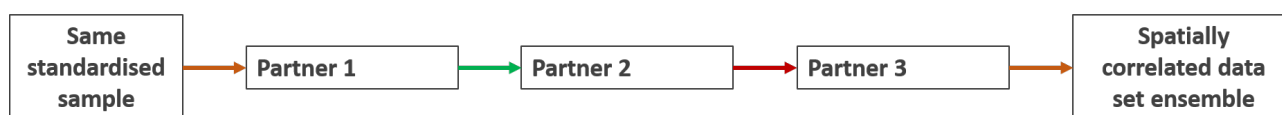


Figure 7. Fully sequential workflow enables spatial correlation

With the intention of overcoming the limitations of the previous two patterns, we have conceived two new patterns, referred to as composite workflows (*cf.* Figure 8 and Figure 9). These blend elements from both of the aforementioned approaches to achieve more effective and versatile experimental strategies. These composite patterns, simple and more complex, respectively (depending on the number of partner interactions and number of steps), are given here as examples. The simple edition (*cf.* Figure 8) focuses on two steps; the first is a set of parallelised experiments, followed by a second sequential step for spatial correlation. Such a workflow allows a wider choice of techniques in step 1 as long as they are compatible with the next experiments in step 2. For instance, one can imagine several lab techniques covering differing properties in a fast / high-throughput and low / mid-fidelity process in the first step. Then, the samples (or a selection of the most interesting samples in the case of high throughput experiments) can be passed on to a Large-scale Scale Facility (LSF) for relatively lengthy but high-resolution and high-fidelity measurements either as confirmation or to complement the previous measures through spatial correlation on the same physical sample(s). The convergence of the sample(s) from various step 1 experimental methods to one (or a selected small number) of step 2 techniques can be designed to improve coherence and/or complementarity to the dataset ensemble. The more complex edition (*cf.* Figure 9) is already a lot closer in the form of a fully deployed and complexified workflow as opposed to a conceptualised pattern. It can be viewed as an amalgamation, combining aspects from the previous three approaches, and can be tailored to specific requirements that need to be addressed. In short, the starting point is still a set of parallelised experiments that may benefit from sending their outputs/samples to a further technique to add or improve spatial/physical correlation, and so on and so forth over several subsequent possible steps. This will strongly depend on the particularities of the selected experiments but, above all, on the characterisation/properties needed to answer the specific scientific question(s).

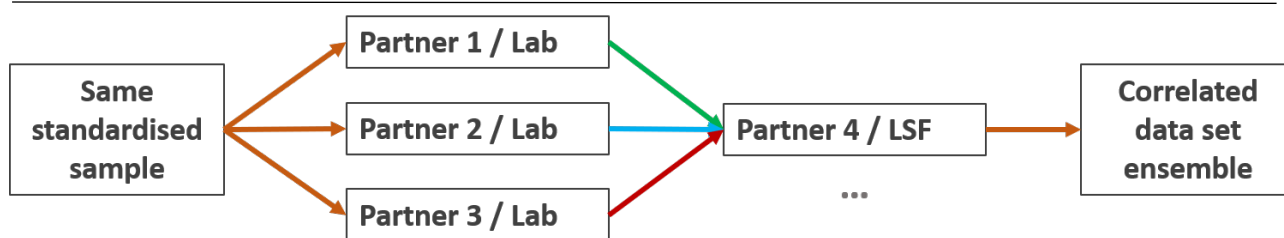


Figure 8. Composite workflow

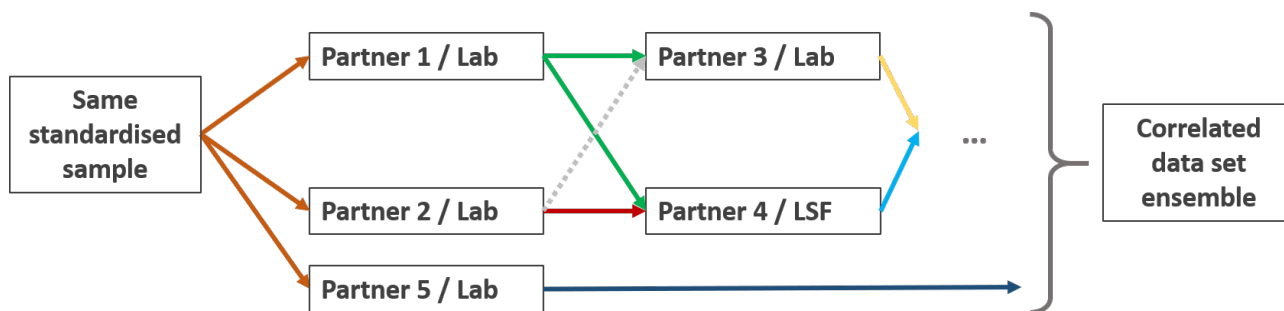


Figure 9. Complex composite workflow

3 Practical workflow application in the scope of D5.3

3.1 Global workflow overview

To design the D5.3 experimental workflow, sample, technique, and organisational modalities have been carefully identified. The choice has been the fruit of an in-depth process, including discussions with all WP5 partners and between WP4, WP5, and WP6 partners.

3.1.1 Motivations

The primary factors influencing this workflow stem from two key considerations. Firstly, batteries are a complicated system to investigate. Numerous properties interplay in their behaviour, and this requires a wide array of experimental techniques from a large range of research fields to perform a complete study. Consequently, it is not feasible for a single expert to master all facets of battery characterisation; instead, it necessitates a collaborative effort of many experts within the community. Based on our experience, as outlined in section 2.1.1, we have realised that this community effort cannot simply involve every field expert focusing independently on their specific area of research. Such an approach does not facilitate a consistent, final correlation of data, notably due to reproducibility issues, along with other factors. Secondly, from section 2.1.2, we realised that standards and protocols are an essential and effective requirement for reproducibility in single-site scenarios. However, they might have a more limited impact, reproducibility-wise, when considering a more complex multi-site and multi-technique framework. Thus, it is imperative to enhance these standards and protocols, with a focus on standardising the sample origin as much as possible. An example of one approach towards this goal is to choose a single partner responsible for producing the samples for a specific workflow. On the scientific front, despite BIG-MAP's focus on electrode interface properties, we made a deliberate decision in D5.3 to not exclusively concentrate on techniques investigating SEI and surfaces. This choice was motivated by our desire to construct a comprehensive overview of our selected cell chemistries, hence recognising that knowledge of the



bulk and overall context is crucial for gaining a complete understanding of the smaller scales involved in interface studies.

The practical workflow used here for the demonstrator aims at exemplifying its applicability, *i.e.*, its technical feasibility, and we will not focus on its scientific outcomes, which will be the subject of subsequent publications.

3.1.2 Samples

Within this demonstrator, we gathered a large set of techniques and collected a large ensemble of datasets. In WP5, during the first part of BIG-MAP, we focused on Tier 1 materials and techniques, *i.e.*, mostly pristine materials like LNO and graphite with the standard BIG-MAP electrolyte, and explored the possibilities offered by the techniques in the D5.1 experimental matrix.

To further develop the science case in D5.3, we shifted interest onto the so-called Tier 2 samples (right part and B insert in Figure 2). This involved aged and standardised electrodes (LNO and graphite). This point alone was already interesting, but by partnering with WP4 and WP6, we also decided to include a selection of improved materials and additives they studied. For instance, LiTDI as an electrolyte additive seemed very interesting due to its demonstrated improvement in cycle life for NMC811 cells and other Ni-rich materials (see Annex 5.2). The Tier 2 experiment materials are thus LNO||Gr aged electrodes at 80 % State of Health (SoH) cycled with or without LiTDI as an electrolyte additive. These samples can, of course, also be compared to the pristine ones where relevant.

In our efforts to achieve sample uniformization, we drew upon the experience gained from cycling large batches of cells by collaborating with partners CIDETEC and FZJ from WP4 and WP6. It was agreed that they would be the providers for the workflow samples, and they then collaborated closely to synchronise protocols for cell assembly, cycling, and disassembly, based on WP8 standards. This aspect is further described in section 3.2.1.

3.1.3 Experimental techniques

For the Tier 2 experimental techniques, we selected those tested during the Tier 1 experiments that could answer most of the scientific points of interest (see Figure 10 and Figure 11) specified by WP5 and BIG-MAP partners. We then built the workflow accordingly. An overview of these different scientific points of interest, along with the related experimental techniques and involved partners, is shown in Figure 10. The points of interest are centered on Li heterogeneity, morphology, electronic structure SEI, and surface, amongst others. The objective was to obtain as global an overview as possible of the electrode properties by aggregating the results at the end. We will not comment on the scientific results here, as this is not the main focus of this report, but some details are given in section 3.3. Figure 11 offers a graphical overview of the raw (or pre-processed) data outcomes obtained from all techniques in the D5.3 workflow, along with the associated observables that collectively contribute to the comprehensive picture we have assembled.

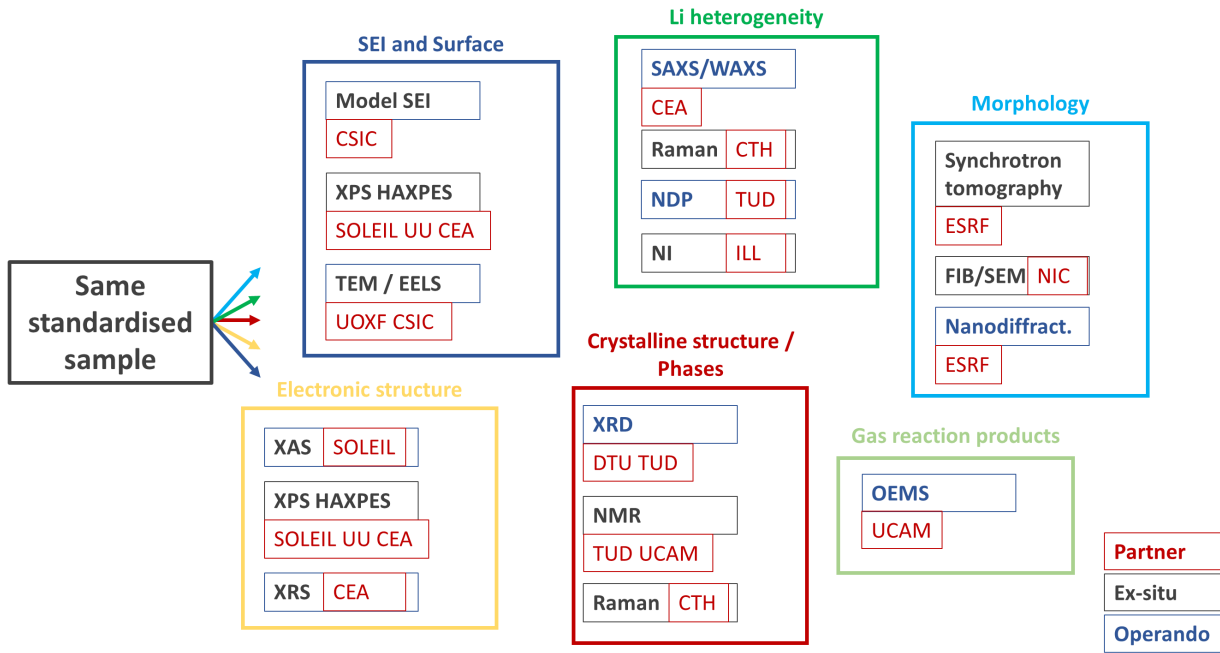


Figure 10. All experimental techniques and the scientific points of interest they are covering along with the involved WP5 partners. A glossary for the experimental technique name abbreviations can be found in Annex 5.1.

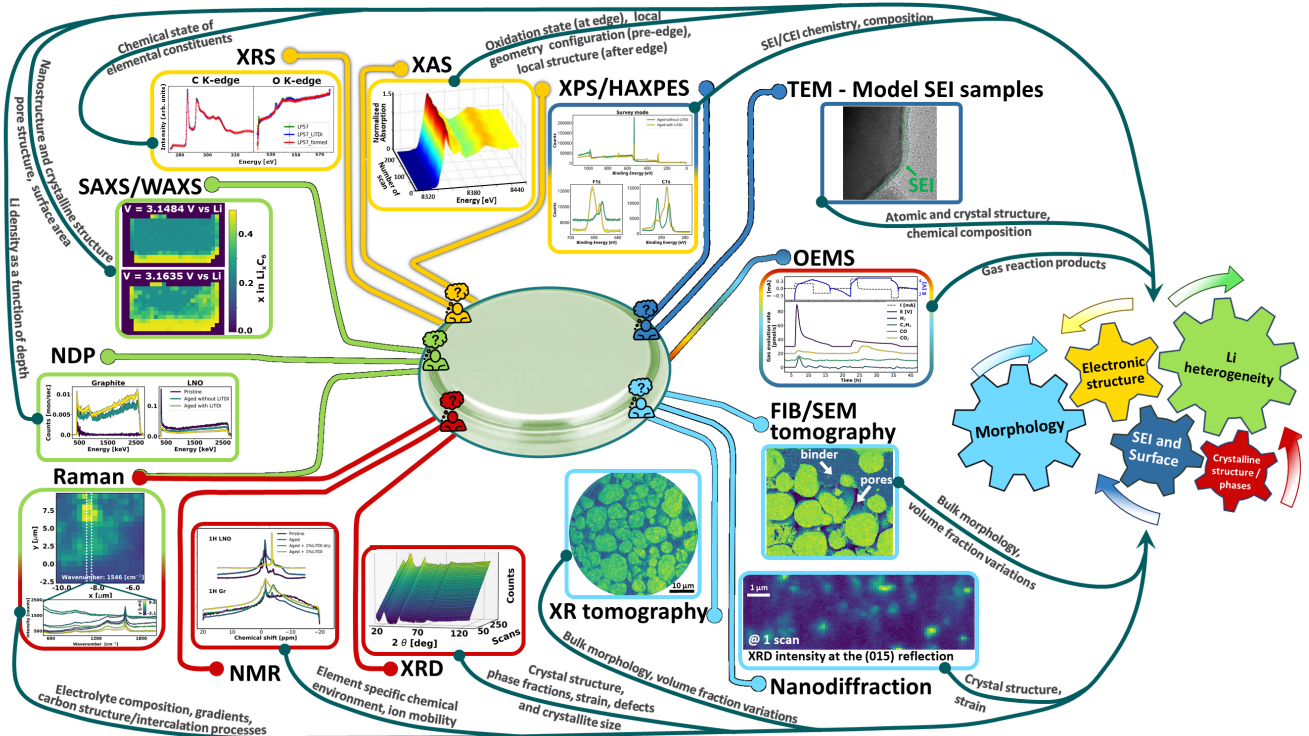


Figure 11. Overview of all techniques used in the D5.3 workflow. Central to this work, and the Figure, is the standardised sample (a coin cell for this workflow). For each technique, colours correspond to the different scientific points of interest introduced in Figure 10. Along with each technique is displayed a snapshot of the characteristic raw data. Key observables obtained after data analysis are described for each technique. Our unique workflow brings together all of these techniques, contrasting and complementing their observables over different scales. A glossary for the experimental technique name abbreviations can be found in Annex 5.1.



3.2 Workflow details

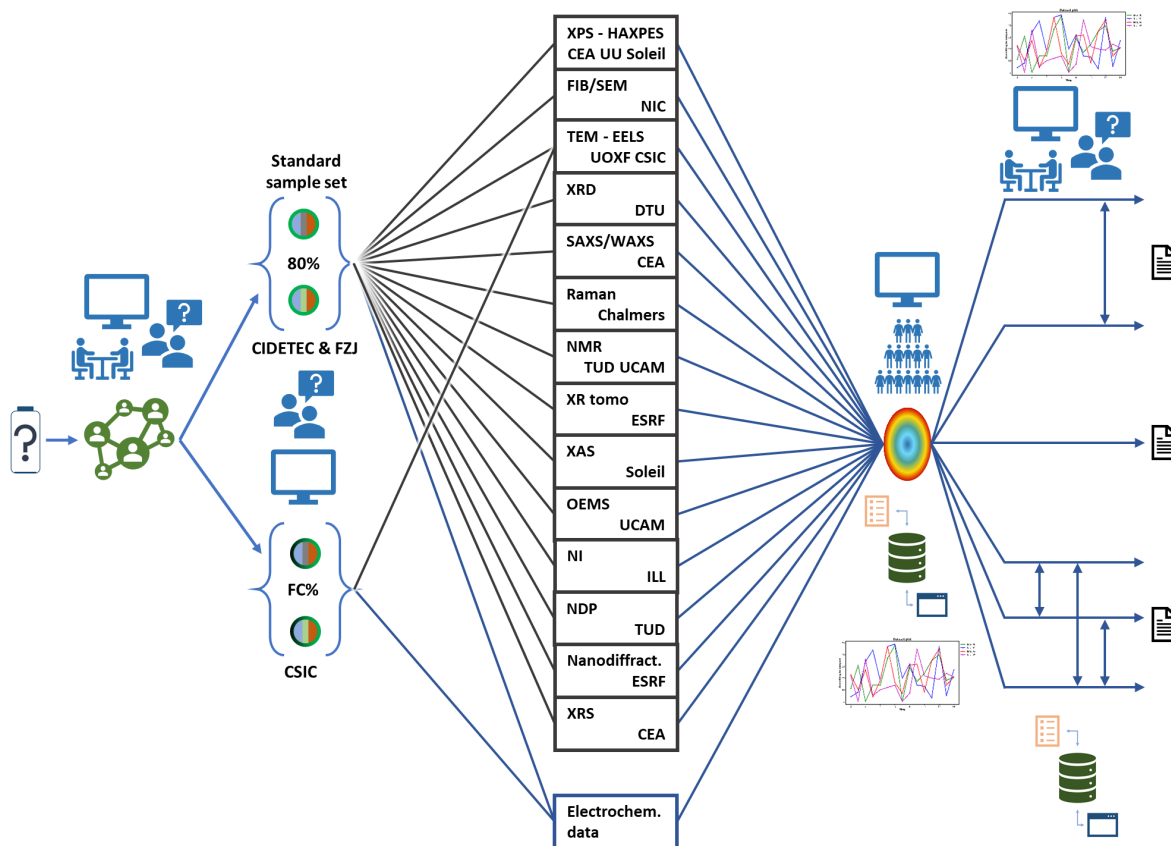


Figure 12. Global view of the D5.3 workflow organisation in a sequential manner; see the Gantt chart in Figure 19 for the timely organisation. FC% means that the cycling is stopped after the formation cycles. Black links symbolize a sample flux while blue represent a data and metadata flux. A glossary for the experimental technique name abbreviations can be found in Annex 5.1.

Figure 12 gives a graphical view of all experimental techniques, organisational tools, protocols, and storage / sharing capabilities that have been leveraged to build and operate the D5.3 workflow. As mentioned in the previous section, we capitalised on the D5.1 experimental matrix and the experiments performed in the first part of the WP5 operation to answer the selected scientific points of interest. Every partner in WP5 has been involved in showcasing, as much as possible, a multi-site and multi-technique aspect. The workflow is designed to mimic the characterisation of new material, employing a broad screening approach to explore various relevant aspects. This is why a combination of ex-situ and a few operando studies has been chosen. The intention is to create a comprehensive picture that serves as an entry point for studying the new material. Such a broad picture enables us to delve into more focused, specific, and short-range characterisation workflows in subsequent investigations.

One can notice that some techniques like XPS and NMR have been performed by more than one partner. This was dictated by a need to check for reproducibility and complementarity, as we have seen from the workflow in section 2.1.2 that XPS and spectroscopic data were not reproducible in these former conditions.

The experimental techniques and their distribution amongst partners form a crucial and visible aspect of the D5.3 demonstration, although they represent a fraction of the entire process. An



equally significant part occurs before the actual experiments, *i.e.*, during the planning and design of the workflow. This process began with identifying the drivers and scientific interests mentioned in section 3.1.

Dedicated group meetings (involving part of or the whole WP5) were organised, when needed, to select the interesting techniques and draft their orchestration inside D5.3. Also, major inputs were the selection of the sample chemistry, detailed in section 3.1, and an estimation of the number of experimental materials (electrode samples from each chosen chemistry and other materials, like electrolytes) required for each experimental set-up. Then the important task of synchronisation related to sample preparation protocols was conducted by FZJ and CIDETEC, ensuring the success of sample uniformization for the workflow. This is detailed in the upcoming section 3.2.1 and was used by CSIC to adapt their in-house protocol for the creation of model SEI samples.

After conducting the experiments, as well as during the workflow execution, ensuring a smooth process relies heavily on information sharing, encompassing both data and metadata. In D5.3, we addressed this challenge by utilising the tools developed by BIG-MAP, such as the BIG-MAP Archive and the BIG-MAP Notebook, along with the tracking of individual samples through persistent identifiers, as elaborated on in sections 3.2.2 and 3.4. These tools were crucial in facilitating effective information sharing throughout the workflow. This is required for future successful result exploitation from D5.3 both within WP5 and the BIG-MAP consortium. Going down this track, WP5 organised in June 2023 an in-person workshop for partners to share their results from the workflow and start detailing further data correlation and complementarity. Discussing these results is outside the scope of this deliverable, but an overview of the scientific outcomes from D5.3 is given in section 3.3.

3.2.1 Battery cycling protocol and sample-providing

To guarantee sample reproducibility, standardised protocols were determined at different levels: (i) cell assembly; (ii) cycling test; (iii) cell disassembly. The protocols at each level are detailed in the next subsections. Each of these standardised protocols is strongly based on the ones issued by WP8, improved by experience feedback from the previous WP5 workflows and know-how from CIDETEC and FZJ.

3.2.1.1 Coin cell assembly

CR2032 coin cells (Hohsen corp. and parts from TOB Xiamen) were assembled in a dry room (-50 °C dew point) following the sketch shown in Figure 13.

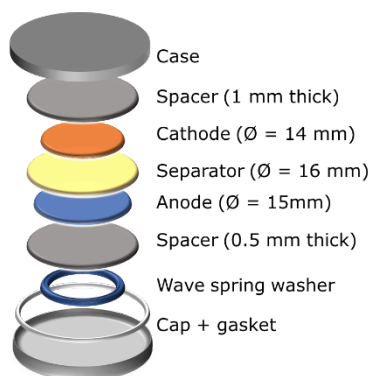


Figure 13. Scattered view of the standard coin cell assembly



First, a gasket, a wave spring, and a 0.5 mm thick spacer were successively placed in the cap. Then, the 15 mm diameter graphite (Gr) anode (CIDETEC, 94 % active material, 3.44 mAh/cm² areal capacity) was positioned on top of the spacer. 44 µl of electrolyte (see below for detail) was added to the cell in two portions. The first portion of 22 µL was gently dropped on the anode with the help of a micropipette. The stack was subsequently covered with the separator (Celgard 2500, Ø = 16 mm), which was then dosed with the second 22 µL electrolyte portion. Then, the LiNiO₂ (LNO) cathode (BASF, 94 % active material, 3.1 mAh/cm² areal capacity, 14 mm diameter) was placed on top of the separator, followed by a 1 mm thick spacer. The assembly was finalised by positioning the coin cell case and crimping the ensemble under an 8 kN force. Concerning the electrolyte (prepared by FZJ), two formulations (in mol/kg for ease of reproducibility) were used:

- 1 m LiPF₆ in EC/EMC (3:7) + 2 % VC, as baseline.
- 0.095 m LiPF₆ + 0.05 m LiTDI in EC/EMC (3:7) + 2 % VC, to check if using the Hückel salt as additive could bring any cell cyclability improvements as hinted by previous studies with NMC (see Annex 5.2).

3.2.1.2 Cycling test

To test the performance of the assembled cells, an ageing protocol was defined based on the following steps from WP8 standards:

1. **Formation step:** 6 h rest followed by three charge (CC step at C/10 followed by a CV step with a cut-off at $I < C/20$) and discharge (CC at C/10) galvanostatic cycles at C/10
2. One galvanostatic cycle, *i.e.*, **initial check-up**, consisting of one CC step at C/20 and one CV step with a cut-off of $I < C/50$, in both charge and discharge, to determine the cell discharge specific capacity at its beginning of life (BoL).
3. **20 galvanostatic cycles** consisting of one CC step at 1C and one CV step until $I < C/20$ in charge and CC step at 1C in discharge to induce accelerated degradation of cells.
4. **One check-up**, as in step 2 to measure the cell specific discharge capacity **and calculate the state of health (SoH)** of the cell, defined as the ratio between the initial and last measured specific discharge capacity.
5. **Repeat 3 and 4 until SoH = 80 %**, when it was considered that the cell reached its end of life (EoL).

During cycling, the operating voltage was fixed in the range from 2.5 V to 4.2 V, and temperature was maintained at 20 or 25 °C. The cell capacities, hence the current corresponding to 1C, were calculated based on the mass of active material and the measured practical capacity of 225 mAh/g.

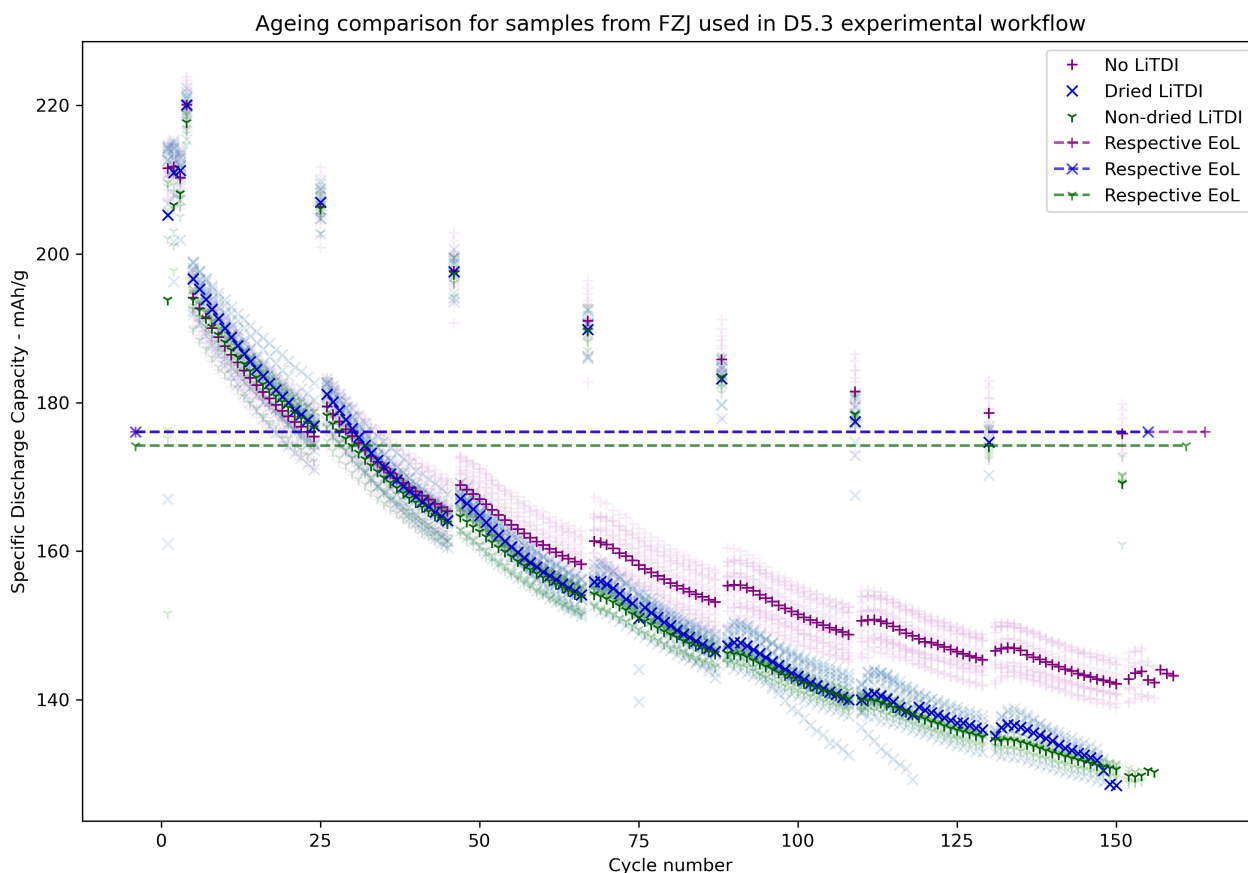


Figure 14. Cycling history comparison for all D5.3 samples. “No LiTDI” designates cells cycled with the standard BIG-MAP electrolyte formulation; “Dried LiTDI” and “Non-dried LiTDI” refer to cells cycled with the modified electrolyte containing LiTDI. The only difference between the previous two series is whether the LiTDI was previously dried or not before making the electrolyte formulation. Each electrolyte formulation is coupled to a colour series, respectively purple, blue, and green. The plain colour markers are for the mean value of the related series, and the semi-transparent markers visualise data from each coin cell in the related series. The horizontal dashed lines mark the respective EoL (80 % SoH) for the mean value of each series, these are superimposed for the purple and blue series.

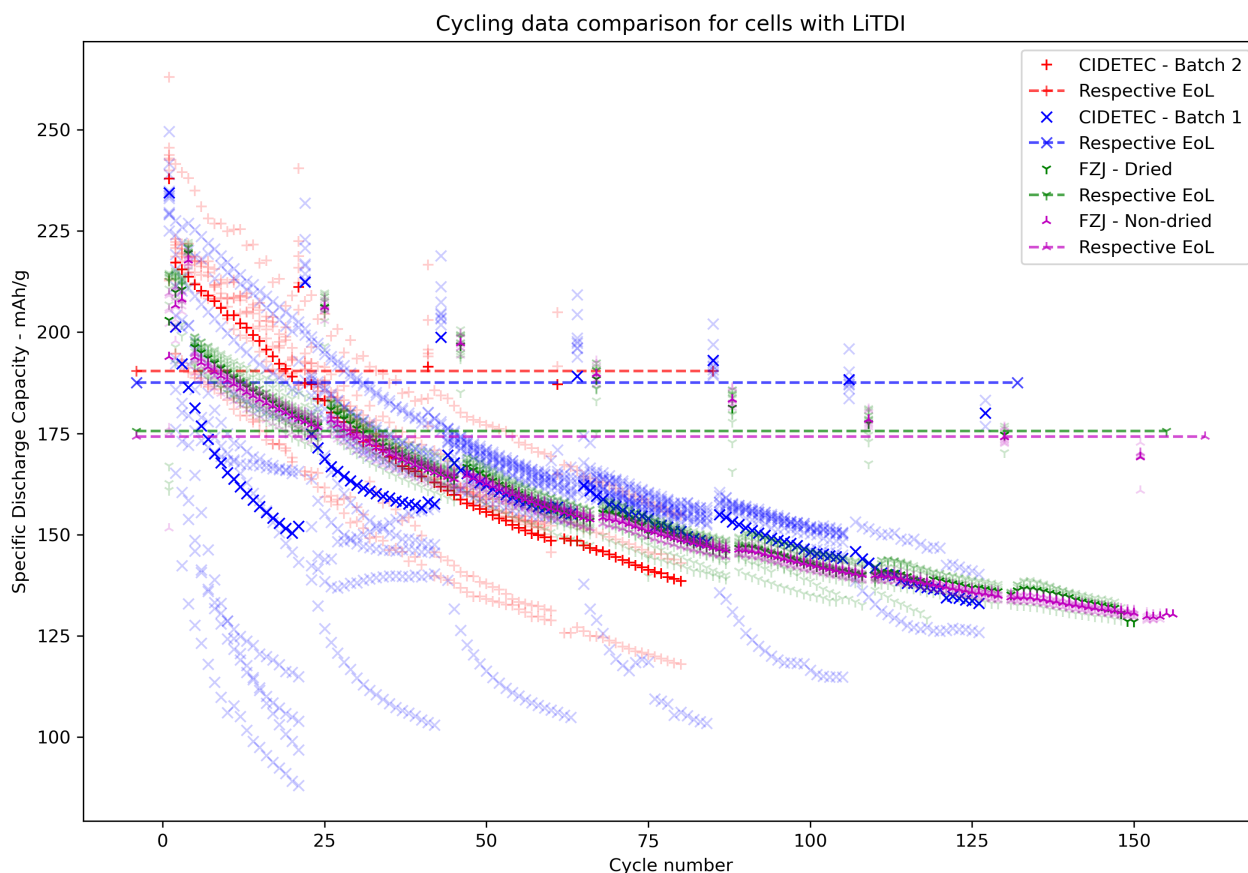


Figure 15. Ageing comparison between CIDETEC and FZJ cells with LiTDI. CIDETEC data is split between two batches, batch 1 in blue and batch 2 in red. FZJ data is split between dried (green) and non-dried (purple) LiTDI, as in Figure 14. The only difference between the two series from FZJ is, respectively, whether the LiTDI was previously dried or not before making the electrolyte formulation. The plain colour markers are for the mean value of the related series and the semi-transparent markers visualise data from each coin cell in the related series. The horizontal dashed lines mark the respective EoL (80 % SoH) for the mean value of each series.

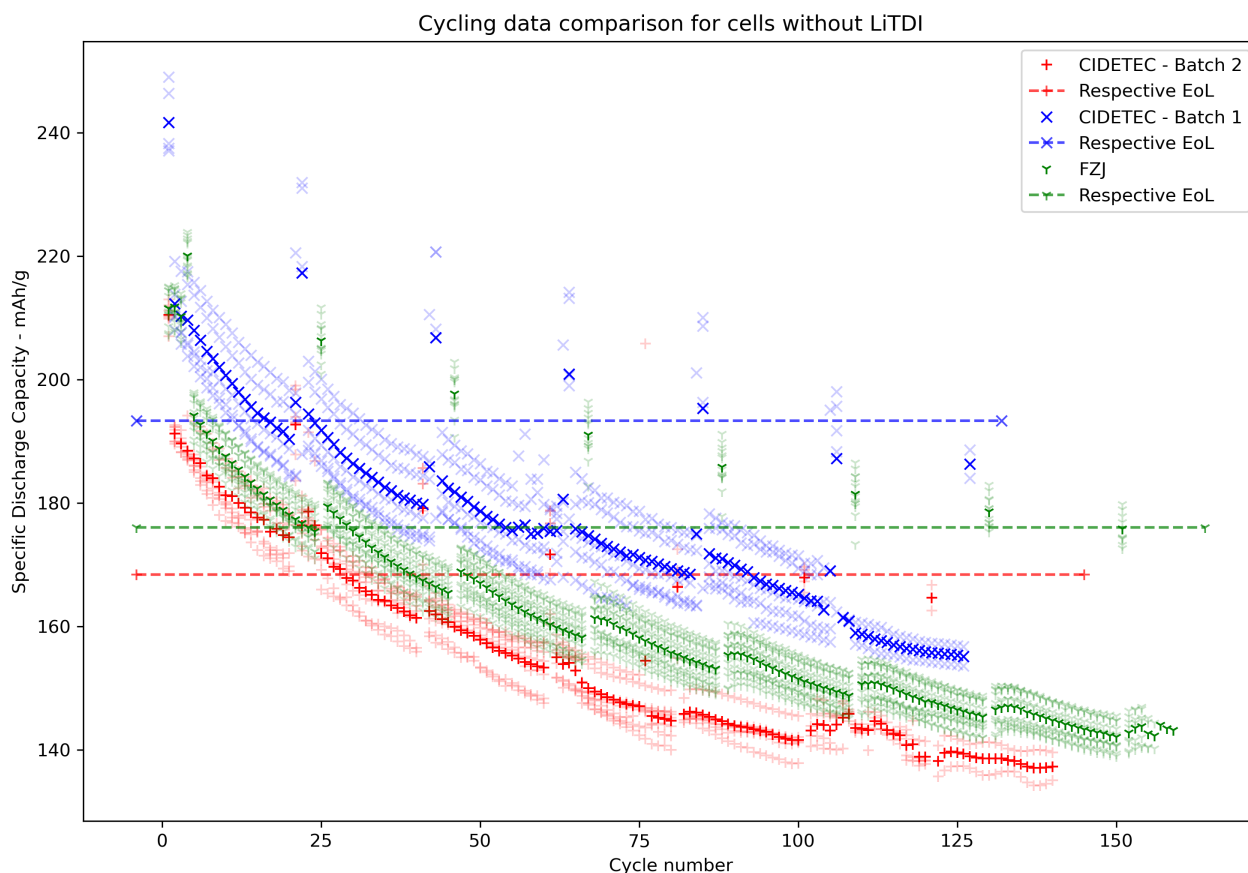


Figure 16. Ageing comparison between CIDETEC and FZJ without LiTDI. CIDETEC data is split between batch 1 in blue and batch 2 in red. The FZJ data series is plotted in green. The plain colour markers are for the mean value of the related series, and the semi-transparent markers visualise data from each coin cell in the related series. The horizontal dashed lines mark the respective EoL (80 % SoH) for the mean value of each series.

Figure 14, Figure 15 and Figure 16 show the aging curves for the cells cycled in the frame of the D5.3 workflow. Figure 14 gathers the aging data from all the cells provided by FZJ that were used in the workflow experiments. Good reproducibility was achieved here with similar mean EoL values within 1 % for the two LiTDI series and similar mean capacity values within 5 % for all series. Figure 15 and Figure 16 are, respectively, comparing cycling results between CIDETEC and FZJ from cells containing or not the LiTDI as an electrolyte additive. The first batch of cells containing LiTDI from CIDETEC shows a higher spread around mean in the individual values that were corrected in the second batch.

Based on the number of cycles, the total amount of time required to create an aged sample from the coin cells proved to be around one month. As a general rule, each coin cell was attributed a unique identifier, thus allowing us to track down which one was used in which experiment (see section 3.2.2 for more details).

We consider that we have achieved a reasonably good reproducibility between CIDETEC and FZJ¹. For each cell chemistry, the EoL values are similar within 10 %, the same is achieved for the mean capacity values on average. As a matter of fact, despite the established and followed protocols, one has to consider that there may exist many reasons that may lead to the observed deviation in the

¹ See for example: Brandon R. Long *et al* 2016 *J. Electrochem. Soc.* **163** A2999, 10.1149/2.0691614jes



final electrochemical result reproducibility, even from one similar coin cell to another. Explanations for this could be:

- Defects arising from cell assembly, such as a misalignment of cell components;
- Small variation in the percentage of active material between electrodes punched from the same sheet owing to the distribution of electrode components (active material, binder, and conductive additives) that, locally, may slightly change from nominal value as a result of the electrode manufacturing process.

3.2.1.3 Coin-cell disassembly

Once the cells reached the EoL, they were opened and disassembled inside an inert Ar-filled glove box, with O₂ and H₂O levels below 0.1 ppm and 0.5 ppm, respectively, to harvest the electrodes. To remove any trace of electrolyte salt, while reducing to a minimum the modification of any solid electrolyte interphase (SEI) and / or cathode electrolyte interphase (CEI) eventually formed on anode and cathode surfaces, electrodes were soaked in EMC for approximately 30 s, decanted and the soaking repeated a second time. It is essential to carry out this process as soon as the cycling is completed to ensure the preservation of the electrodes in the desired state. Leaving a coin cell unopened and stored for a few months can lead to additional degradations due to unwanted reactions occurring inside the cell during storage. After this step, the electrodes were sealed inside the glovebox in aluminium-laminated bags to avoid any moisture contamination during sample delivery.

3.2.2 Sample repartition and delivery with data tracking

When developing and coordinating a multi-site and multi-technique workflow, particularly at the EU scale, it is crucial to not only plan the required number of samples in advance but also to carefully consider the logistical aspects of sample procurement and distribution. This is especially true in this context, as one partner is providing all the workflow samples. The logistical aspect holds significant importance as a fundamental component of sample history and tracking. In fact, both reproducibility and interoperability are contingent upon the effective transmission and storage of identifiers, as well as accurate data and metadata management throughout the sample entire scientific life cycle.

Figure 17 illustrates the conceptual approach adopted during D5.3 to address this part of the organisation. Here, we identified two different paradigms, the first one focused on the physical sample and the “material plane”, and the second is centred around the datasets generated from the physical sample with all the associated metadata and numerical enablers. The sample providers (FZJ and CIDETEC) gave each cell a sample ID that propagated to the constituting electrodes and was communicated to the experimental partners during the sample shipment. Then the partners performed their experiments, generating one or several datasets with their related metadata. The metadata were then added as an entry in the BIG-MAP Notebook and the datasets as a record in the BIG-MAP Archive. The electrochemical data and metadata from the sample ageing are also stored this way. Both tools provide a unique identifier (doi / url) for each entry or record and ensure online availability and sharing both within WP5 and the entire consortium. The BIG-MAP Archive additionally allows to attach tags to a record improving its searchability through the user interface or the API. The usage of both the BIG-MAP Archive and the Notebook are discussed in the scope of D5.3, in section 3.4.

Table 1 gathers information on the different sample shipments including the recipient partner, the parcel reception dates and contents along with the experimental techniques these samples were



devoted to. The time orchestration of the D5.3 workflow will be discussed in more details in section 3.2.3. To complement this information, Figure 18 displays the physical sample flux in D5.3. Most of the samples have been provided by FZJ for practical reasons as they had enough samples to provide for the entire workflow. Some samples were also delivered from CIDETEC at the very beginning of the workflow for timing reasons and by CSIC as they designed a specific model sample preparation to complement the data that would be obtained through TEM measurements on the standard aged samples.

From a very practical point of view, the shipment delivery time (using mostly DHL or UPS services) were tracked to be between 2 to 15 days with an average around 8 or 9 days. This delivery time does not seem to be strongly dependant on the distance between sender and receiver. As an example, we could observe that Soleil (located in France near Paris) received packages 5 days earlier than CEA (located in France, Grenoble) from both CIDETEC (Spain) and FZJ (Germany). We also unfortunately have to report the non-zero probability of a lost parcel as one from CSIC to UOXF was reported missing, introducing delays and the necessity to make modifications to the experimental plan. Concerning shipment costs, one shipment is reported to be around 15 to 30 € depending on the partner, parcel type and delivery provider. Usual package cost reported by FZJ is 19.65 € per physical package.

These points might seem like minor details, or common sense, but they need to be considered to ensure the smooth running of such complex workflows and a long-term understanding of the collected data.

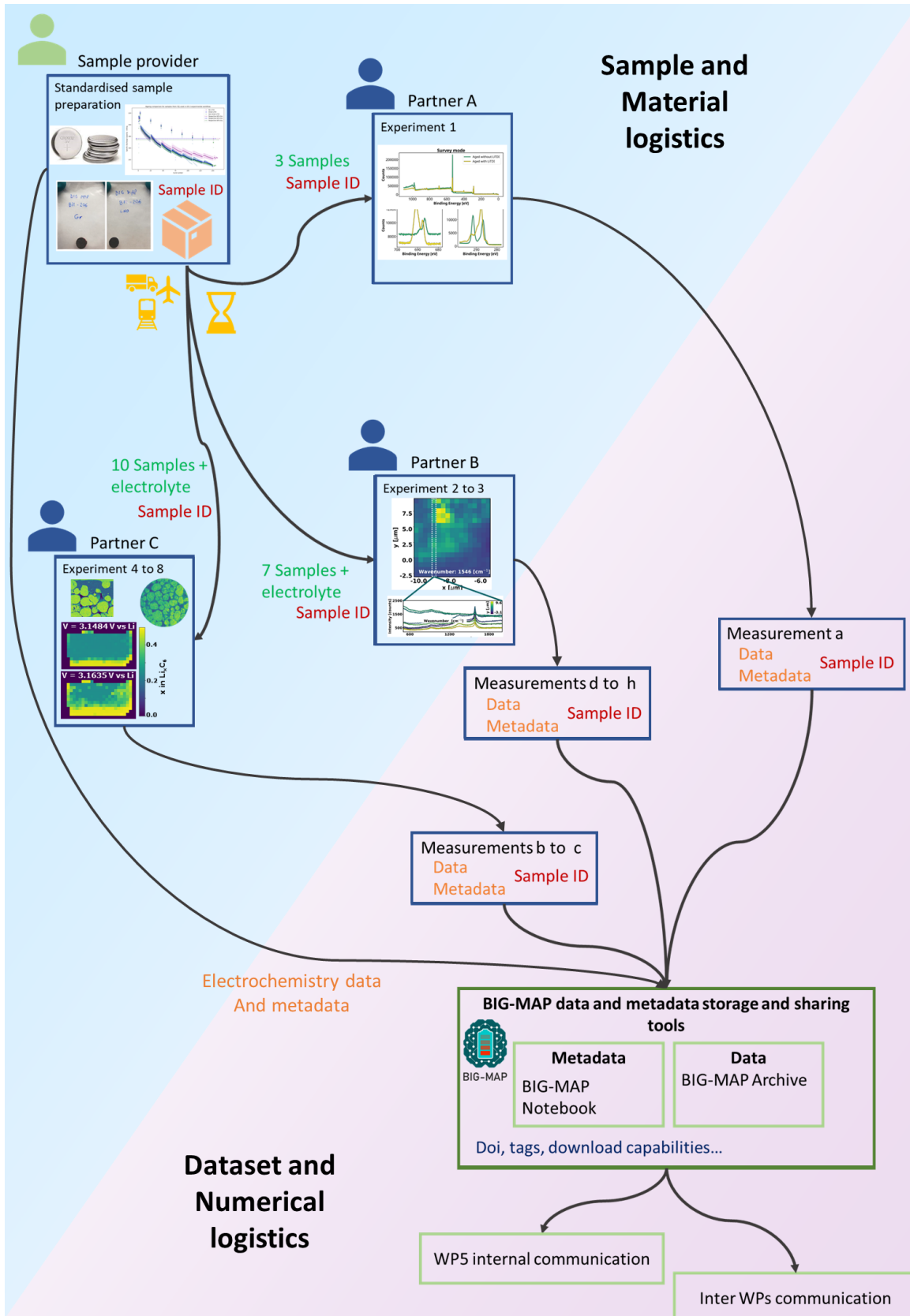


Figure 17. BIG-MAP D5.3 logistics, conceptual view. Two different paradigms, although intricately linked, are showed here. On the top left is the material area with physical samples, parcels, shipping possibilities... On the bottom right is the numerical area where we consider datasets, associated metadata and cloud storage and sharing capabilities developed during the BIG-MAP project.

**Table 1. Summary preview: experiments, samples received and parcel delivery per partner. Rows are sorted by sample reception date.**

Partner	Sample reception	Number of samples received				Experimental technique
		LNO aged	Gr aged	LNO + LiTDI aged	Gr + LiTDI aged	
CEA	Oct 22	-	-	0.5	0.5	XPS
Soleil	Oct 22	-	-	0.5	0.5	HAXPES - LSF
UU	Oct 22	-	-	0.5	0.5	XPS
CEA	Nov 22	1	1	0.5	0.5	SAXS / WAXS - LSF
ESRF	Dec 22	0.5	-	0.5	-	Nano diffraction - LSF
ESRF	Dec 22	1	1	1	1	X-Ray tomography - LSF
DTU	Dec 22	-	-	3	3	XRD operando
Soleil	Dec 22	-	-	1	1	XAS - LSF
CEA	Dec 22	1	1	1	1	XRS - LSF
Chalmers	Dec 22	1	1	1	1	Raman mapping
CEA	Dec 22	0.5	0.5	-	-	XPS
UU	Dec 22	0.5	0.5	-	-	XPS
TUD	Jan 23	2	2	2	2	NMR
UOXF	Jan 23	0.5	0.5	0.5	0.5	TEM – EELS
ILL	Jan 23	1	1	1	1	NI
NIC	Jan 23	1	-	1	-	FIB/SEM tomography
TUD	Jan 23	1	1	1	1	NDP
UCAM	April 23	1	1	1	1	NMR
UCAM	April 23	2	2	2	2	OEMS + pristine samples
CSIC	-	-	1	-	1	* Making model samples for SEI study using TEM-EELS
CSIC	-	-	1	-	1	* ¹ TEM on CSIC samples (originally intended to be performed in UOXF)

*No experiments performed on aged samples from FZJ or CIDETEC but actually working with in-house developed protocols to get model samples for SEI analysis under the TEM (EELS compatible). These samples were also designed for complementary TEM experiments at UOXF but not performed due to some unsolvable issues. The experiments were *in fine* performed at CSIC (¹)

LSF means Large Scale Facilities.

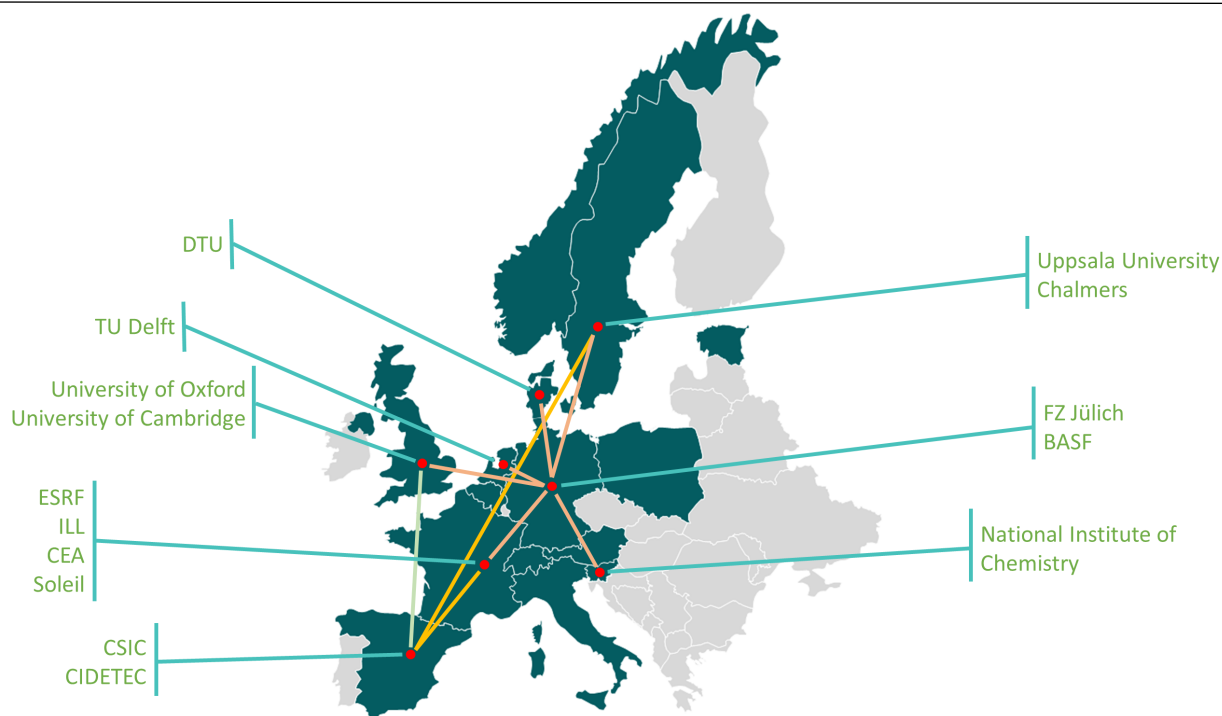


Figure 18. BIG-MAP D5.3 geographical sample flux. In yellow are samples sent from CIDETEC to CEA and UU, in pale orange are samples sent from FZJ to all designated partners and in pale green are the samples sent from CSIC to UOXF.

3.2.3 Timely orchestration of D5.3

Figure 19 shows the final timeline of the D5.3 experiments in a Gantt chart along with the sample shipment date from FZJ and CIDETEC. This workflow was officially launched during a WP5 plenary meeting on 30th September 2022. With the exception of the TEEM-EELS measurements at UOXF, that could not be completed due the instrument status and availability issues, all other experiments have been carried out successfully. This is an excellent result to report as a demonstration of the capability of the BIG-MAP WP5 to run a coordinated multi-site, multi-technique and multi-scale matrix of experiments.

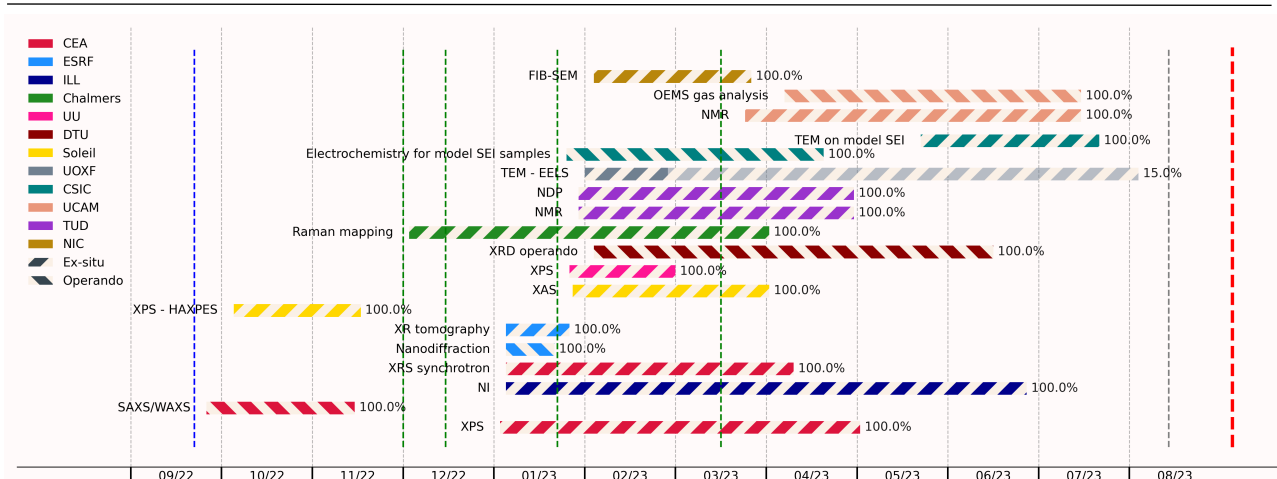


Figure 19. Final Gantt chart for the D5.3 work organisation. The dashed vertical grey and red lines are the deadlines for the present deliverable report (respectively internal and contractual). The blue vertical dashed line materialises the sample sending by CIDETEC. The green vertical dashed lines are showing the different sample sending dates from FZJ. Percentages and bar colour completions are symbolising the current experimental completion as of 07/08/2023. Bars for experiments start on sample reception and end once the experiment is performed when the task is completed (plain colour and 100 %) otherwise it starts on sample reception and end on an arbitrary date with plain colour and percentage indicating the task completion.

The task (experiment) bars represent the time elapsed between sample reception at the partner’s facility and the end of the experiment. In the case where the experiment has not been completed (the progress bar is not entirely in plain colour and associated percentage not at 100 %), the bar is set to end at an arbitrary date and the plain colour fill and percentage track the task completion.

Figure 19 includes a sample shipment by CIDETEC slightly ahead of the launch date (a few days before) to comply with access to the LSF experiments that were already planned.

From the analysis of this plot, we can highlight that there is a delay between the sample reception and the experiment completion of typically one to four months. This stands true for both LSF and lab-scale experiments, without significant difference between these. The fact that this delay is not significantly longer for LSFs (in comparison to lab experiments) is due to proper ahead-of-time planning and secured access to LSF thanks to WP5 partners and long-term proposals. Without this approach, *i.e.* should we had not secured the access to the LSFs, we would have been required to follow the proposal acceptance process scheduled every 6 months, resulting in a total waiting time of approximately 1 year between the initial planning and the actual experiment realisation. We can also remark that the samples are usually rapidly delivered, with one exception that is obviously due the Christmas and New Year holiday period.

The cumulative experimental time (represented by the total bar length) and the shipment duration (considering the longest delivery time for each shipment date) amount to approximately 54.5 months and 1.8 months respectively. This is reported here in the span of the roughly 10 months of execution that necessitated the D5.3 workflow. This is a considerable duration and a parallel framework definitely saved some overall execution time. These times do not include the 5 months of preparation, planning and organisational time that were needed to build and design the workflow before its kick-off.



3.2.4 Organisational points to discuss

As discussed briefly in the previous sections, certain unforeseen events can occur that will disrupt the seamless operation of a workflow.

- The loss of a parcel. It happened once during D5.3 execution with the parcel from CSIC to UOXF. This caused some delays in the TEM analysis of these samples and forced to repeat the sample creation step. It also had for consequence that the TEM measurements on these model samples were finally conducted by CSIC and not UOXF.
- Instrument unavailability or maintenance. As an example, some experiments were delayed because of the overbooked schedules of some instruments, the necessity of planned maintenance or unforeseen technical breakage (e.g. FIB/SEM tomography at NIC and TEM-EELS at UOXF).
- The human aspect. Particularly when the designated contact person for the experiments becomes unavailable due to reasons such as illness, time-limited contracts, or other factors. This situation can lead to delays during the transition period, as was the case for the XRD operando experiments at DTU.

The majority of these issues had minimal impact in the development of D5.3, primarily due to the mostly parallel nature of the workflow. The experienced delays and setbacks would have been much more detrimental in a more sequential workflow as exemplified by the situation with the model samples from CSIC. Quite obviously, in a sequential framework, the workflow would have required five times more time to complete, and we would have lost any spatial correlation from the parcel loss. This illustrates the adaptivity benefits from a parallel (or mostly parallel composite) workflow in the scope of such a wide range screening investigation.

3.3 Scientific outcomes

Herein, we expose a first analysis of the outcomes extracted from D5.3 as a workflow, the first ever demonstration of the capability to run coordinated multi-technique experiments to acquire multi-scale data applied to a selected chemistry. The following analysis offers a “meta-view” of the demonstrator results aiming at emphasising the strengths and weaknesses of the workflow on D5.3 scientific outcomes. In practice, a survey (see form in Annex 5.3) was sent to the experimentalists in order to collect the first conclusions from their experiments. Typical questions were defined by the nature of the samples selected for the Tier 2 experiments, *i.e.* the impact of the cell ageing and / or addition of LiTfDI in the electrolyte from the point of view of the electrode physical and chemical properties (morphology, SEI, Li concentration and the other scientific points of interest mentioned in section 3.1). This analysis can be used at a later stage to identify potential collaborative areas and practical insights for the development of future workflows. This higher-level perspective may even contribute valuable practical knowledge for the construction of the key demonstrator KD4; an essential part of the future WP5 workflow builder.

Figure 20, Figure 21 and Figure 22 show the “meta-view” extracted from the D5.3 experimental results. A global aggregating view and some subset views can also be found in Annex 5.4. The analysis extracts three primary axes from the outcomes: scientific points of interest that have clear and robust answers, those that remain uncertain, and those that appear to exhibit diverging answers.

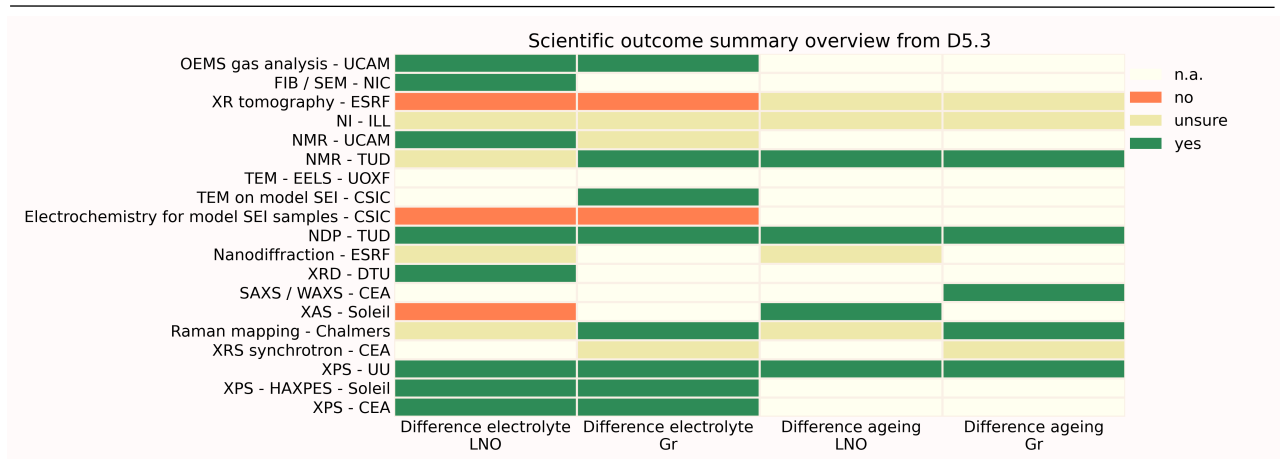


Figure 20. Overview summary for the scientific outcomes from D5.3. The grid colours answer the question, “is there a difference caused by ...”, n.a. means not applicable. For example, in column “Difference electrolyte LNO” and line “XPS - CEA” the cell is green, which means that significantly different XPS spectra between LNO electrodes cycled with and without LiTDI have been obtained by CEA.

Figure 20 focuses on the general effect of ageing and cycling with LiTDI on both LNO and Gr electrodes. Generally, most techniques found differences (green colour), some techniques are “unsure”, and a few found no differences. Regarding the “unsure” techniques, this is due to challenging or time-consuming data analysis (nanodiffraction operando, XR tomography and NI). While the large majority of green suggests that most of the chosen techniques are sensitive to electrode changes during cycling, confirming the good choice of techniques, the question related as to why certain techniques did not observe differences induced by cycling electrodes with LiTDI (vs. without LiTDI) is apparent. This can be readily explained by the fact that we are dealing with a diversity of techniques probing different length scales or chemical / physical properties. Some of these techniques are also performed ex-situ and other operando, which adds another potential difference.

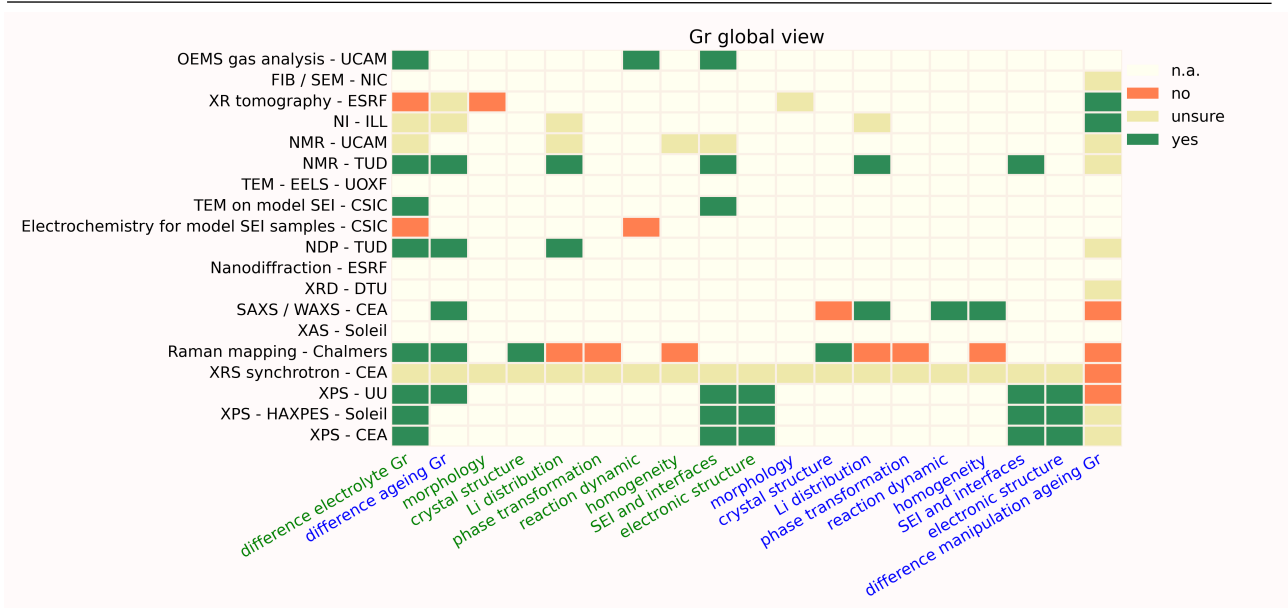


Figure 21. Global view of D5.3 scientific outcomes concerning the graphite negative electrode. The scientific points of interest related to the electrolyte formulation are identified as the green abscissa labels and the ones related to ageing as the blue abscissa labels. The grid colours answer the question, “is there a difference in ...”, n.a. means not applicable. For example, in line “Raman mapping - Chalmers” and column “Li distribution” written in blue, the cell is orange, which means that no noticeable differences in Li distribution for Gr electrodes have been obtained using Raman mapping by Chalmers when comparing aged and pristine electrodes.

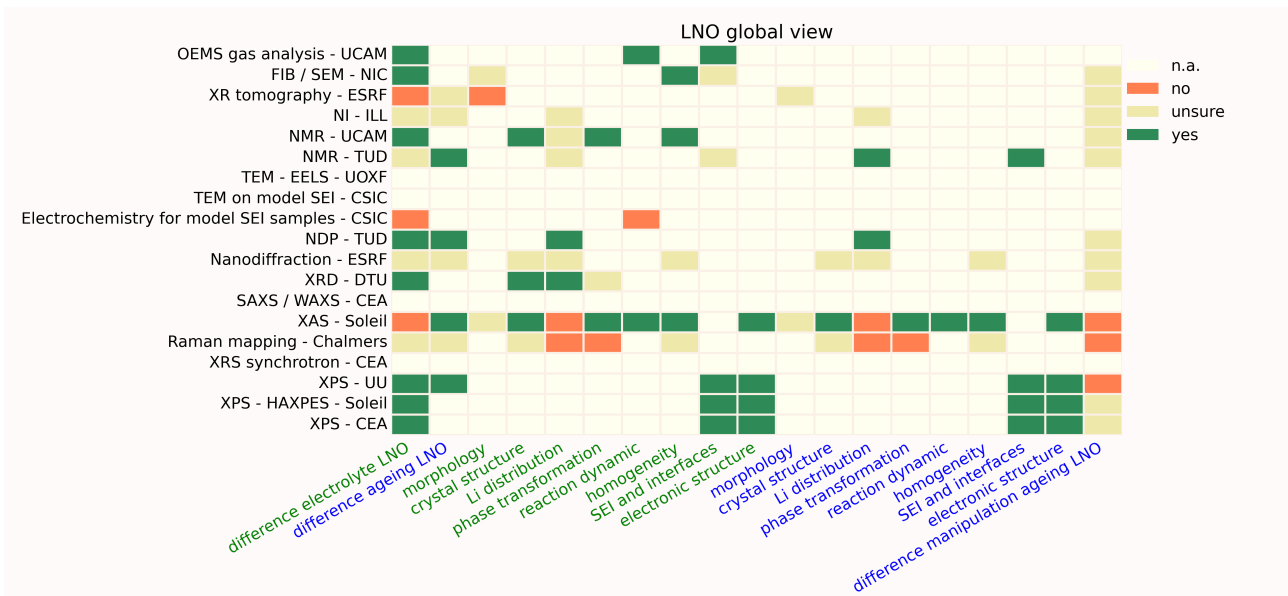


Figure 22. Global view of D5.3 scientific outcomes concerning the LNO positive electrode. The scientific points of interest related to the electrolyte formulation are identified as the green abscissa labels and the ones related to ageing as the blue abscissa labels. The grid colours answer the question, “is there a difference in ...”, n.a. means not applicable. For example, in line “Raman mapping - Chalmers” and column “crystal structure” written in green, the cell is in beige colour, which means that the experimental result interpretation (from Raman mapping performed by Chalmers) is unsure about differences in homogeneity for LNO electrodes when comparing cells cycled with and without LiTDI as an electrolyte additive.



Figure 21 and Figure 22 (and Annex 5.4) show more detailed results focussing on the scientific points of interest for the graphite negative electrode and the LNO positive electrode respectively.

The two scientific points of interest that have yielded weaker (uncertain) results are related to identifying the morphological changes induced by ageing in both the LNO and Gr electrodes (column 11 in both figures). This can be attributed to the fact that quantitative changes are not readily apparent in the tomography and XAS datasets. These observations require more precise quantitative analysis to reach a more conclusive answer.

Ten points resulting in seemingly divergent outcomes are observed. Two of them concern the changes in the reaction dynamics induced by LiTDI in both LNO and graphite electrodes (column 7 in both figures). This can be explained by the fact that OEMS and XAS are respectively looking at gas reaction products and electronic structure variations during cycling, whereas the electrochemistry for model SEI samples refers to the cycling when creating the model samples. These are totally different observables thus there is no contradiction in the differing behaviour. In fact, the electrochemistry being similar when creating the model samples with the different electrolytes is encouraging as this is in good agreement with the extensive cycling performed for sample production by CIDETEC and FZJ (see section 3.2.1.2).

The other points (Li distribution and phase transformation changes caused by LiTDI and ageing in LNO electrodes - columns 5, 6, 13 and 14 in Figure 22 - and crystal structure, Li distribution and homogeneity changes induced by LiTDI and ageing in graphite electrodes - columns 4, 5, 8, 12, 13 and 16 in Figure 21) apparently put at odds various combinations of SAXS / WAS, NMR, NDP, lab operando XRD, XAS and Raman mapping. A reason for this could be the spatial scale difference, as operando XRD give information averaged over the entire electrode when NMR and NDP average on small amounts and XAS looks at smaller areas or even a few LNO particles as does Raman mapping. The difference between XAS and Raman, that have similar scales, is due to the fact that XAS focused on inter-particle differences while Raman mapping aimed at intra-particle variations. For the Gr electrodes, the differences mainly involve SAXS / WAXS and Raman mapping. This time the variations most probably come from the scope and scale of the studies. SAXS / WAXS was used to resolve heterogeneities in the electrode thickness operando (averaging in plane) and the Raman mapping scanned mostly intra-particle variations, only looking at a few particles at the surface layer of the electrode.

Two additional very positive aspects can be gleaned from the information. First, the XPS results show good reproducibility, a definitive improvement in comparison to the workflows performed previously to D5.3. Second, there is a number of scientific point of interests that are answered by several (converging or otherwise) techniques from different fields (with potentially different observables and scales) - a positive indication that correlated analysis will bring new valuable insights thanks to high complementarity.

From a practical feedback perspective, it is intriguing to observe that aging does not appear to introduce significant difficulties in handling the LNO electrodes. In contrast, certain imaging techniques show differences in the case of the graphite (Gr) electrodes. Specifically, aging seems to render the Gr electrodes more fragile, making them more challenging to handle without incurring damage.



3.4 On the use of the BIG-MAP Archive and BIG-MAP Notebook

To ensure the usefulness of the experimental data collected in a complex workflow such as D5.3, it is necessary to use some centralised and standardised storage and sharing tools for data and metadata. In the scope of BIG-MAP, these tools are the Notebook and the Archive.

The BIG-MAP Notebook, developed within WP8, organises and stores the experimental metadata. It has ontologised entries according to the WP7 BattInfo ontology which makes it ideal as all recorded fields have a homogenised meaning.

The Archive is the BIG-MAP centre for storing and sharing datasets whether they result from simulations or experiments. To analyse the use of the BIG-MAP Archive records created from the D5.3 demonstrator, we collaborated with WP9 to develop automated capabilities. The current section reports the information extracted using this feature as of 07/08/2023.

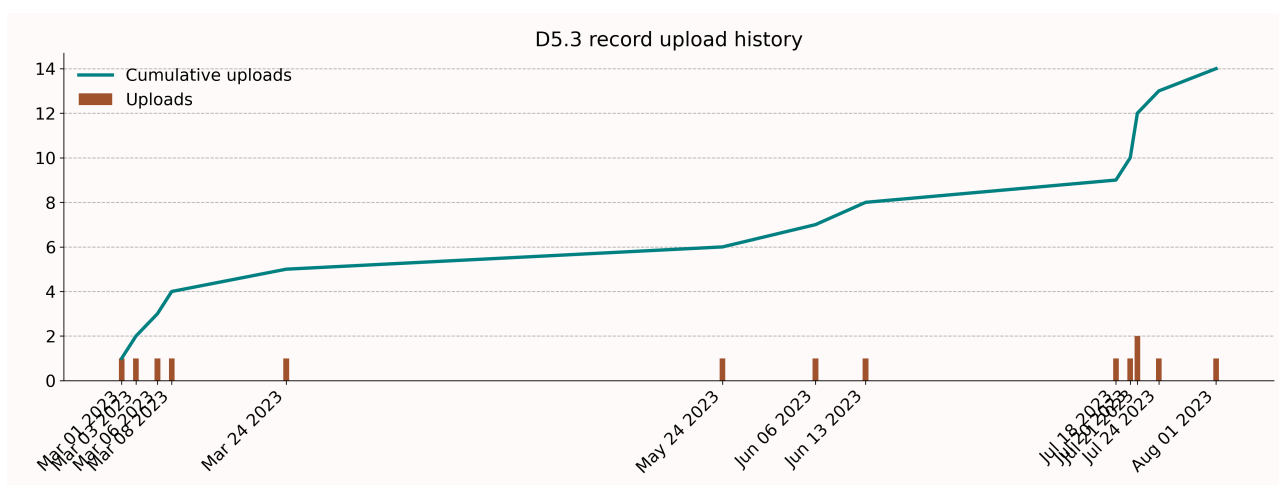


Figure 23. Upload history in the BIG-MAP Archive for the experiments related to the D5.3 workflow

Figure 23 displays the upload history of records related to D5.3. While a good number of records, 14, have already been created in the Archive, it does not amount to the total number of records one could expect from D5.3, which is 21 (19 counting one record per experiment, *cf.* Figure 26, plus one from both FZJ and CIDETEC with the sample electrochemical data). While we have 2 records for the Raman mapping from Chalmers (one for both the LNO and graphite electrodes), the two inputs from CSIC are merged into one single record, which evens the count, resulting in a filling completion at around 67% for the BIG-MAP Archive. However, some of the collected datasets are still under analysis and more records will be added in the future.

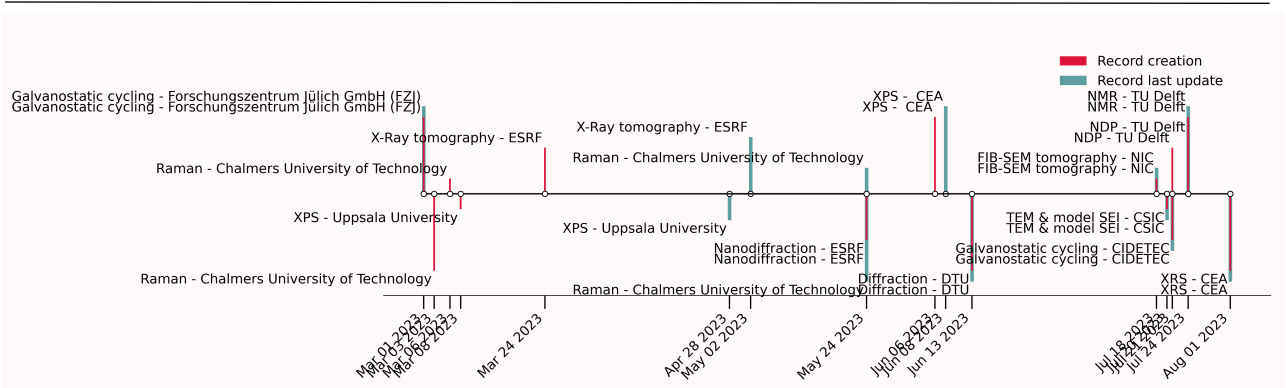


Figure 24. Timeline for the BIG-MAP Archive usage related to the D5.3 workflow. Record creation (last version) is in red and last update in blue. Matching length and orientation are used to link the markers for the creation date and last update date pertaining to the same record. Corresponding partner and experimental technique are also attached to each marker.

Figure 24 reports the record creation and related last update dates for each of the records created during D5.3 execution. It is encouraging to see that some of the records have been updated after their creation, signifying that they are actively maintained and used by their creators.

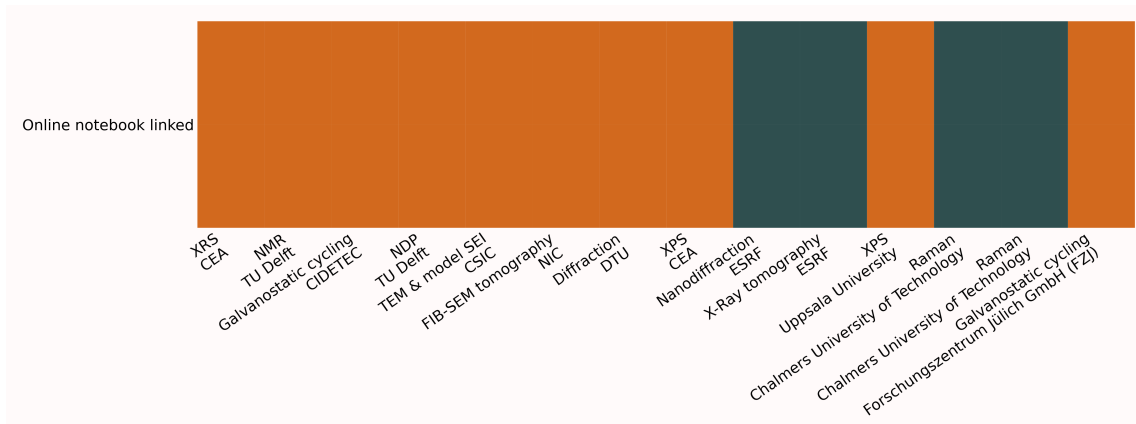


Figure 25. Integrated links to the metadata in the BIG-MAP Notebook for the D5.3 related records in the BIG-MAP Archive, green is yes, orange is no.

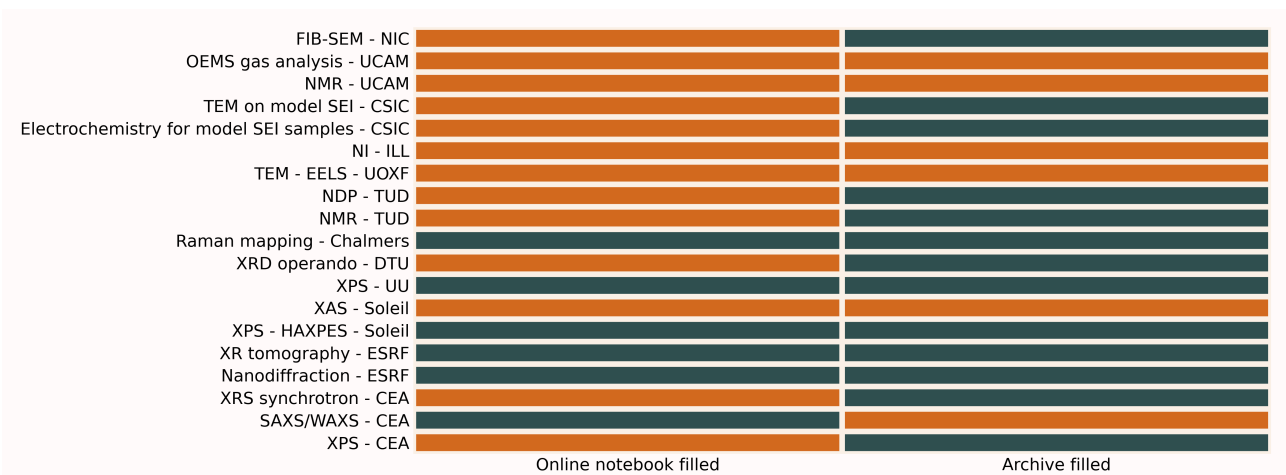


Figure 26. Status for filling the BIG-MAP Notebook and Archive regarding the experiments in the D5.3 workflow, green is yes, orange is no



BIG-MAP



Figure 25 and Figure 26 report, respectively, if the Archive record contains a link to a related Notebook entry and if a record or entry has been created for the D5.3 experiments. At the time of the writing of this report, the BIG-MAP Archive contains more up-to-date records than the BIG-MAP Notebook, and further records will be created in the very near future, after completion of data analysis or reduction processes still pending. The status of the BIG-MAP Notebook use is not as positive. Some of the partners encountered problems when creating their accounts or entering metadata for performed experiments, thus preventing the creation of some entries. Moreover, as filling the entries cannot be automated through an API and it basically needs one manual entry per sample, especially for electrochemistry, which causes some delays in adding more entries for D5.3. These last two points would need improvement to increase the efficiency and utility of the BIG-MAP Notebook, particularly for large scale workflows.

Figure 27 and Figure 28 respectively showcase the estimated number of visits (views) and the estimated total number of downloads per record related to D5.3 shared on the BIG-MAP Archive. It should be noted that if there are multiple files to download in a record, their number of downloads are added up here. Please, refer to Annex 5.5 for a visual of the estimated number of downloads per file in each record. These records, as well as their related datasets, are showing their usefulness through a certain number of visits and downloads. The record displaying the highest number of visits and downloads is containing the cycling electrochemistry data from FZJ. This is interesting as it is related to most of the samples provided for all experiments in D5.3, and as such its highest utility is understandable. The record concerning the XPS data at the CEA has also been consequently visited and used. It was also used for a workshop exercise on data analysis - further details regarding this will be provided in D5.4. One thing to point out is that the records showing no recorded dataset download are very recent as per the update date for the data in the current section (cf. Figure 24) which can explain this state.

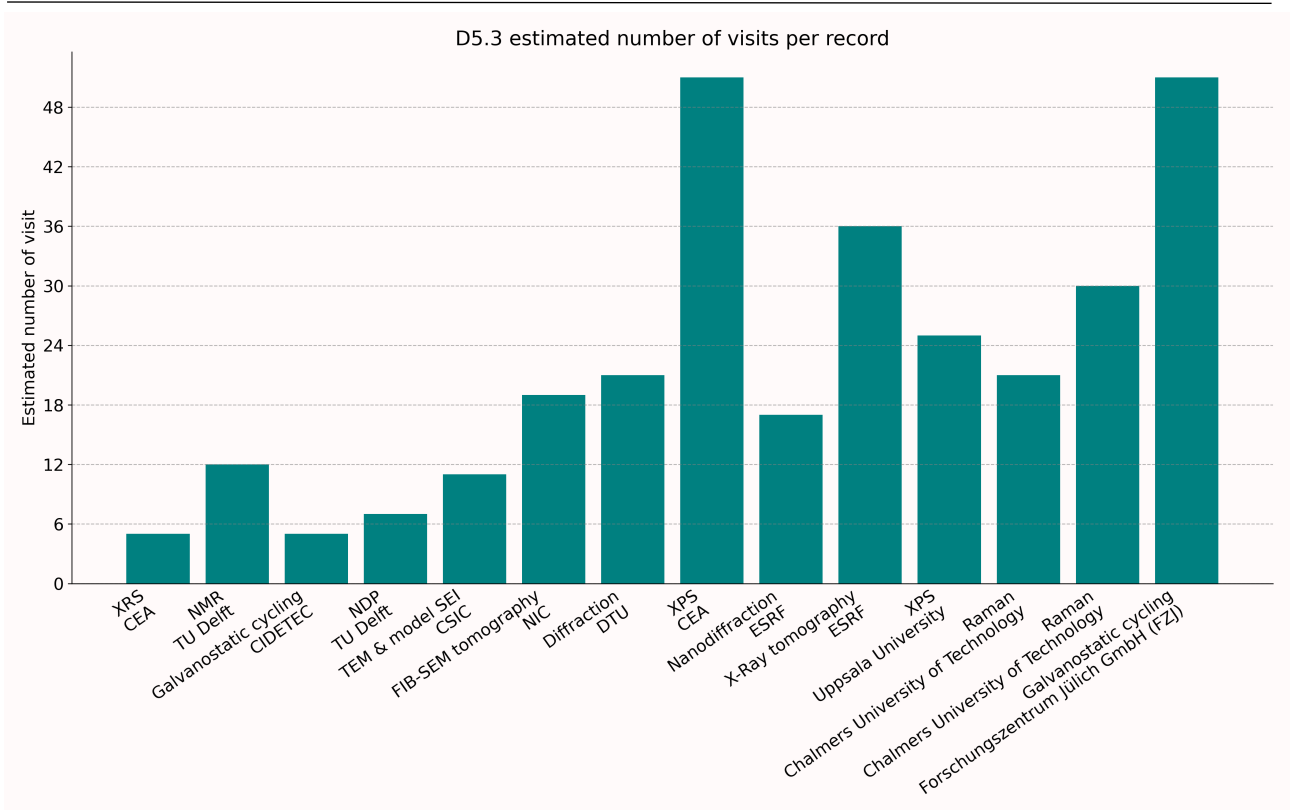


Figure 27. Estimated number of visits per record linked to D5.3 and shared on the BIG-MAP Archive

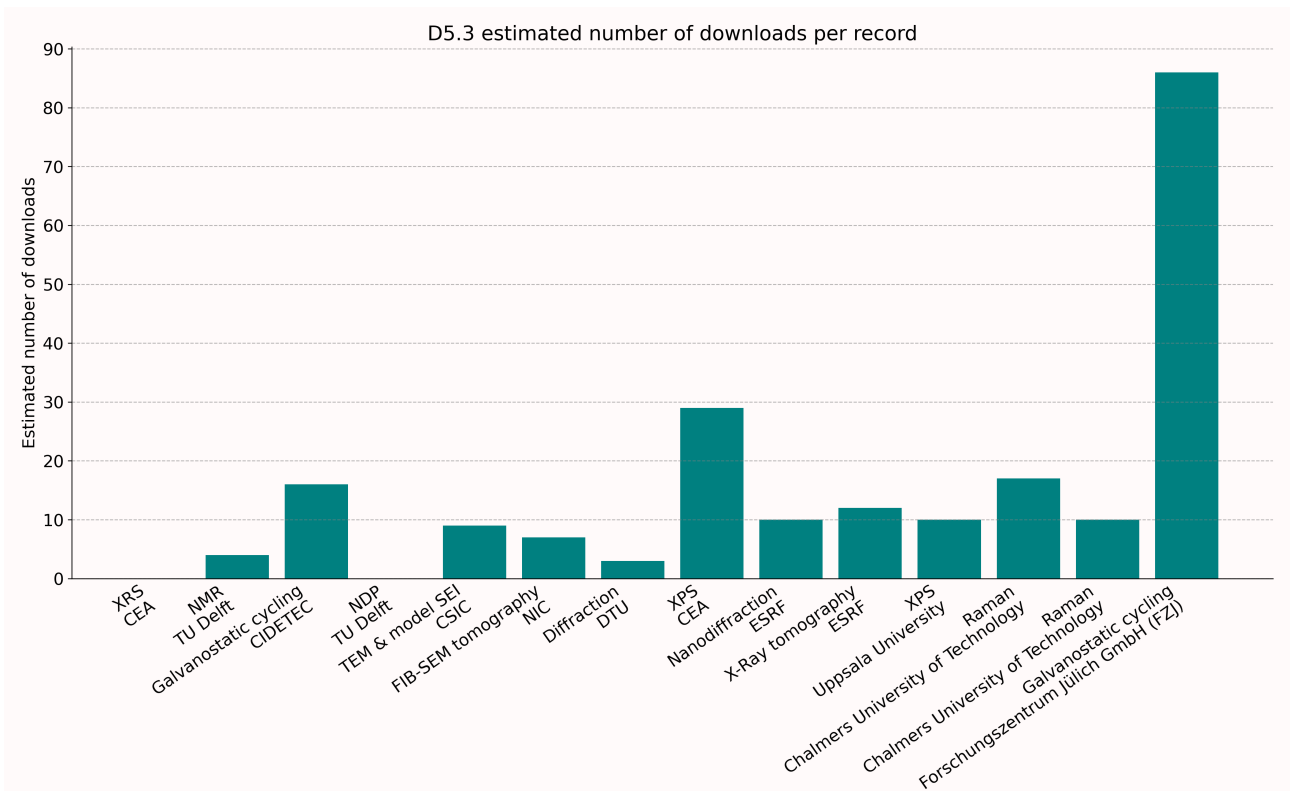


Figure 28. Estimated total number of downloads per record linked to D5.3 and shared on the BIG-MAP Archive



3.5 On-the-fly visualisation and pre-processing of experimental data

On-the-fly visualisation and pre-processing of experimental data are critical in most research areas. They allow the real-time monitoring of the experiment, facilitating control over any experimental issues or equipment malfunctions, enabling immediate assessment of the quality and validity of data, allowing timely interventions if any irregularities are detected, and helping making decisions about the experimental setup and environment.

In battery research, on-the-fly visualisation is particularly necessary during operando experiments, allowing the monitoring of the electrochemistry of the cycling battery and experimental data, enabling scientists to make immediate decisions. Nevertheless, several battery characterisation techniques need to pre-process the data in order to correctly visualise it.

Experiments within WP5 have been conducted at both laboratory and LSF scales. Most of the partners already used specific (possibly in-house) software, if available, before the beginning of BIG-MAP to visualise and pre-process the raw data. If these tools were not available beforehand, they were developed within WP5. Simplified data can be straightforwardly visualised, and WP5 partners used software packages such as Python, Matlab or Oracle towards this end.

In the following subsections, we first discuss the need for visualising the electrochemistry of the cycling battery during operando experiments. Then we present two specific techniques for which semi on-the-fly visualisation and / or pre-processing raw data algorithms were developed.

3.5.1 Electrochemistry data

Operando experiments are of utmost importance in battery research, as they enable us to observe and investigate real-time processes occurring during battery cycling. During these experiments, batteries are cycled using a potentiostat, a specialised instrument that precisely controls the voltage or current throughout the cycling process. The *EC-Lab*² software is the most common electrochemical control and analysis software amongst WP5 partners. On-the-fly visualisation of electrochemical data itself is implemented in *EC-Lab*.

Visualising electrochemical data during battery cycling is essential. It allows for continuous monitoring of battery performance, ensuring prompt detection of any anomalies or unexpected behaviour. This timely awareness enables researchers to take necessary interventions, such as adjusting experimental conditions (modification of the C-rate, decide whether or not to continue cycling, etc.), or promptly spotting and replacing faulty cells. It also aids in monitoring various aspects of cell performance, including capacity, voltage profiles, cycling stability and SoH.

3.5.2 Visualising raw data at LSFs

LSFs have specialised needs when it comes to data acquisition and raw data visualisation. The high number of instruments at each LSF, and the large datasets produced, has prompted the development of specific software and interfaces to efficiently manage their complex operations and unique requirements. Depending on the technique, the software may allow on-the-fly visualisation of raw data.

² <https://www.biologic.net/topics/ec-lab/>



BIG-MAP



For instance, at the ILL, the instrument control system, called NOMAD, connects to each of the servers running on the instrument computers and interacts with them in real-time. For many of the instruments, on-the-fly raw data visualisation can be done directly with NOMAD allowing scientist to assess the experimental setup and data quality. These include the powder diffraction D2B and D19 instruments, the SANS D22 instrument and the NeXT instrument in neutron imaging mode, all used in BIG-MAP.

At the ESRF, diffraction, scattering and tomographic techniques were used. The nano holotomography technique on ID16b unfortunately does not allow for automated on-the-fly visualisation of the raw data. This technique scans the sample in multiple projected images (radiographs), producing very complex data that needs to be processed altogether to reconstruct the 3D volume. The most akin to decision assisting pre-processing is the visualisation of one slice in the partially reconstructed data which can aid in determining if the imaged area is significant or not in addition to the radiographs used to centre the sample in the beam. For the scattering techniques like SAXS/WAXS on ID31 or XRS on ID20, the beamlines provide a suite of scripts and utilities for data reduction that can be run during the beamtime, helping to check pre-processed data from the previous step during an experiment. Nanodiffraction data from ID01 requires specific treatment to be processed into meaningful observables. Nevertheless, on-the-fly visualisation of raw integrated data for SXDM (Scanning X-Ray Diffraction Microscopy) mapping is available on the beamline and can help to see if the crystal of interest is still in the scanned area or not. Pre-formatted Jupyter notebooks, making use of an in-house developed Python module for data analysis, are also available and can help to run some data reduction to estimate the observables in a time frame compatible with decision making during a beamtime.

At the Soleil synchrotron, the *DataBrowser* software package can be used to manually browse and visualise the raw data stored in a Nexus format. There is not a unique software to visualise and pre-process raw data from all beamlines.

In the following, we will discuss two specific semi on-the-fly data visualisation and pre-processing tools developed within BIG-MAP.

3.5.2.1 ROCK beamline for XAS experiments at Soleil

The ROCK beamline at Soleil specialises in X-ray Absorption Spectroscopy (XAS) and is primarily used for characterising catalysis and battery materials. At this beamline, raw data is acquired and subsequently processed by the instrument scientists to perform data normalisation and energy calibration. This calibration is experiment dependent, as it varies based on the sample being studied.

For operando battery experiments, a scan number and a time stamp are associated to the stored raw data. However, in order to track and correlate the battery evolution with the electrochemistry, it is necessary to jointly visualise the electrochemical and experimental data.

To achieve this, the ECXAS algorithm was developed in Python to aggregate electrochemical and experimental data together. This is done in a semi on-the-fly fashion because the raw data still requires manual normalisation and calibration before aggregating the data. The ECXAS algorithm is publicly available in GitHub³, and installed at the ROCK beamline, easily accessible through a Jupyter

³ <https://github.com/GhostDeini/perex>

notebook. Although EXAS was developed for the ROCK beamline, the aggregation algorithm could be also used to aggregate data from other beamlines or battery techniques.

Figure 29 illustrates an example of the visualisation capabilities offered by EXAS. It showcases a 3D plot of XAS spectra over time, where the correlation with cycling potential data is color-coded, making it easily comprehensible.

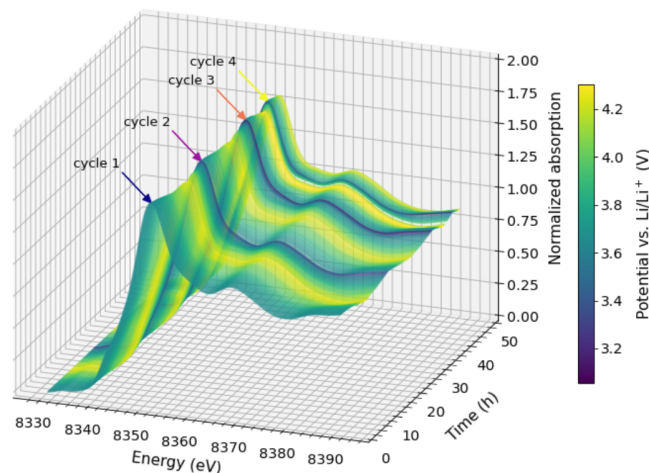


Figure 29. 3D visualisation of XAS data obtained at the ROCK beamline (Soleil) by EXAS after aggregating the electrochemical data with the experimental data.

3.5.2.2 D2B Neutron powder diffraction instrument at the ILL

D2B, a state-of-the-art neutron powder diffractometer at the ILL, offers exceptional resolution and is well suited to investigate the crystalline structure of anode and cathode materials. Specifically, properties such as the unit cell lattice and atomic site parameters, as well as lattice strain and size, can be probed.

During operando experiments, these material properties may undergo variations, and phase transitions can occur. Real time raw data visualisation becomes crucial as it allows researchers to promptly identify and analyse any changes in the material structure and properties. It also enables on-the-fly modifications of the cycling parameters, if needed.

NOMAD displays the raw data from D2B as a 2D map of the diffraction pattern. This visual assessment allows for evaluating the quality and statistical properties of the data. However, this visualisation is insufficient to follow phase transitions during cycling. To achieve accurate results, raw data requires pre-processing, involving calibration by the detector efficiency and subsequent combination of all NeXus files obtained in one measurement. Then, data needs to be transformed into a 1D diffractogram for comprehensive representation as well as to allow comparison with other data.

We have developed semi on-the-fly algorithms to process and visualise D2B data taken during one measurement. These algorithms also enable the statistical comparison of processed diffractograms to assess any phase modification during cycling.



3.5.2.2.1 D2B DATA

The 2D D2B detector consists of 128 parallel tubes spaced at 1.25° intervals. One acquisition (numor) in D2B consists of a complete 2D diffraction pattern, which is obtained after 25 steps of 0.05° in 2θ . Thus, each numor contains 25 entries that need to be processed together. Such scans are repeated to improve statistics. In "Detector Scan" mode, this is achieved by repeating the acquisition 10 times, with each time the initial θ angle moved by 1.25° so that counts are averaged over several detectors. Consequently, each measurement during an operando experiment consists of 10 different numors, each containing 25 separate diffractograms.

3.5.2.2.2 METHODS

We developed the algorithms in Python using the Mantid Python API. Mantid is the main software for data reduction at the ILL. It is a framework for high-performance computing and visualisation of neutron scattering data⁴. It provides a core framework in C++, a Python API, python plugins and a cross-platform graphical desktop application.

The algorithm consists of two main functions:

- Data processing. *D2Bdatared* is the function to perform calibration of D2B data. It takes the raw data as input, from one to several numors (ten for a typical measurement) and performs calibration using the *PowderILLDetectorScan* Mantid algorithm. The output is a 1D diffractogram which the user can visualise.
- Diffractogram comparison. Once the data is processed, the *Comparison_spectra* function compares two 1D diffractograms. It divides the spectra and compute statistics: χ^2 and standard deviation, and the minimum and maximum values of the division of the spectra. Figure 30 illustrates this comparison.

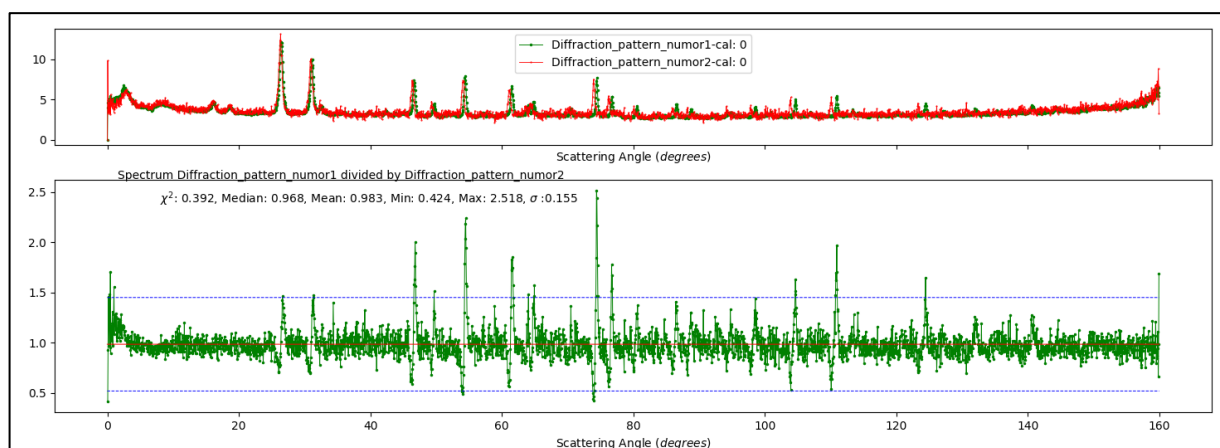


Figure 30. Visualisation of pre-processed D2B data. On top, the overplot of two consecutive 1D diffractograms. On the bottom, division of the two diffractograms, statistical information such as χ^2 and standard deviation, and the minimum and maximum values is also provided.

These two algorithms are intended for interactive use during the operando experiment. Data processing of 10 numors is relatively quick (< 2 minutes), allowing for a statistical comparison of two

⁴ www.mantidproject.org



1D diffractograms in just a couple of minutes. This provides scientists with enough time to decide whether or not any modification to the electrochemistry is necessary.

Additionally, data reduction and 1D diffractogram comparison can be carried out automatically after the experiment is finished, using a specific Python workflow: *automated_datacal.py*. This algorithm reads all raw data from the folder, groups the numors based on whether they were measured together or not and processes the data.

Although the data reduction algorithms are specific to the D2B instrument, the diffractogram comparison algorithms can be used for any kind of 1D diffractogram data.

The algorithms are publicly available in GitHub⁵.

3.6 Experimental operando or in-situ cell harmonisation in WP5 / D5.3

Experimental operando or in-situ cell harmonisation is a very complex subject to tackle as every group traditionally has its own cells, all tweaked from specific needs encountered in previous experiments.

The very first step in this direction in WP5 has been made alongside the experimental matrix in D5.1 under the form of an experimental cell matrix. This experimental cell matrix regroups all the cells available together with description of their characteristics, allowing identification of those that can be used across multiple techniques. The partners reported that both commercial (e.g. Lerich or EI-cells) or in-house developed cells are used. During D5.3, the EI-cell was used for the operando measurements with in-lab XRD and synchrotron nanodiffraction while one Swagelok cell design from CEA was successfully used for operando synchrotron scattering and neutron imaging. This has set the basis for the harmonised cell pool for a common experimental platform.

Additionally, within BIG-MAP, Soleil developed a new experimental cell (see Figure 31). This cell is designed to facilitate reproducibility through ease of assembly, even in a glovebox, and to be compatible with most of the experimental techniques represented in WP5. This was kicked-off by an in-person workshop organised in Grenoble (November 2021) and reported in D5.5. During this workshop partners discussed compatibility and potentials over some preliminary cell designs. One conclusion was that no cell can accommodate every experimental technique and that Soleil's cell should focus on spectroscopic techniques (excluding for example tomographic techniques) both in-lab and at LSFs. A version of the cell was tested and proved to have reliable and reproducible electrochemistry cycling with a standard coin-cell-like structure, making it a user friendly in-situ cell. The cell was tested under real coin-cell conditions (according to WP8 protocols) with in-lab Raman at Chalmers and a combination of Raman and XAS on synchrotron set-ups at Soleil. Although there are some improvements to be made to enhance the compatibility with multiple set-ups, the results show reliable electrochemistry and the potential to run combined experiments both in-lab and at LSFs.

⁵ <https://github.com/cnherrera/automated-data-calibration-d2b-mantid>

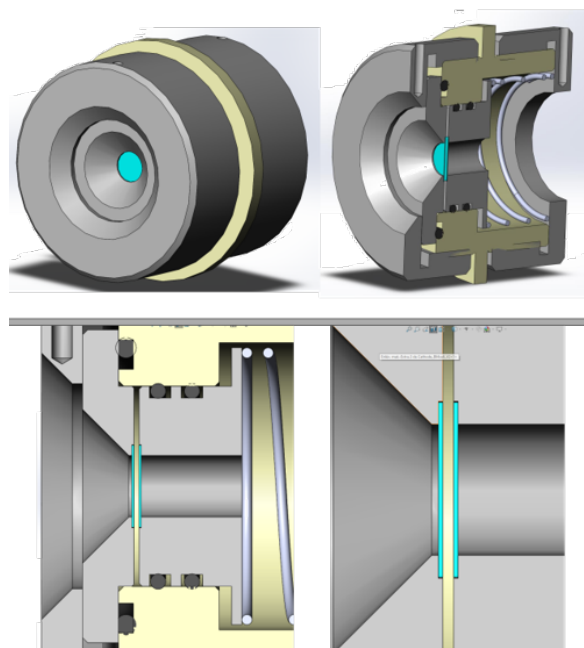


Figure 31. Technical CAD drawings for the new multi-technique experimental cell developed by Soleil

4 Conclusion, outlooks and links to D5.4 and data analysis

In this report, we present the first-ever demonstration of the capability to conduct timely coordinated multi-technique experiments in a pan-European scale, enabling the acquisition of multi-scale data and involving the collaboration of 15 partners gathering research and technology organisations, academic laboratories and Large Scale Facilities. The success of this demonstrator is built on several cornerstones developed in collaboration with the different BIG-MAP Work Packages and more specifically from the work performed in WP5. Effective communication and information sharing amongst the contributing partners have been crucial aspects, and although this was initially challenging, the implementation of good practices eventually led to the establishment of efficient flows.

As a first and main cornerstone, the workflow reported here has proven its effectiveness in successfully characterising the properties of two selected chemistries cycled in a standardised full cell configuration, using multi-site, multi-technique and multi-scale coordinated experiments. The importance of a meticulous definition of a suitable workflow has to be highlighted, as it serves as the backbone for the well-coordinated characterisation campaign.

None of this would have been possible without work dedicated to experimental cell harmonisation and semi-automated on-the-fly tool development for data visualisation and pre-processing.

Another important cornerstone is the use of common tools such as the BIG-MAP Notebook and the BIG-MAP Archive which play a crucial role in facilitating the effective storage and sharing of data and metadata, thus ensuring an efficient correlative analysis of the data.

Relying on standards and protocols from WP8 is also key in insuring reliability and reproducibility in electrochemistry cycling during sample preparation for example.

Data analysis and scientific results were only briefly alluded to as this will be the focus of our upcoming deliverable D5.4 and future publications by WP5 partners.

An essential lesson learned from this work is the critical need for efficient collaborative frameworks to use standardised language (via ontologised tools like BattInfo from WP7) and to follow similar reproducible procedures (by relying on shared tools and protocols) to validate results effectively.



BIG-MAP

Battery Interface Genome - Materials Acceleration Platform



As mentioned before, after the data acquisition step detailed here in D5.3, the next D5.4 deliverable will cover data analysis aspects, stemming from the results generated by this experimental workflow. WP5 also utilised this work as a stepping-stone to initiate a collaboration with the ontology experts in WP7. This collaboration aims to create a new, updated, and ontologised experimental matrix for the key demonstrator KD4.

We firmly believe that the effective work performed in WP5, specifically D5.3, as reported in the present document, has paved the way for the European Battery research community to engage in synergistic collaborative research and development and has initiated the implementation of a European multimodal experimental platform. This collaborative effort is intended to support and contribute to the advancement of the battery industry and Europe's energy transition by fostering the development of next-generation batteries.



5 Annexes

5.1 Glossary for experimental techniques

Electrochem.	– Electrochemistry
FIB-SEM	– Focused-Ion Beam – Scanning Electron Microscopy
HAXPES	– Hard X-Ray Photoelectron Spectroscopy
Nanodiffract.	– Synchrotron X-Ray nanodiffraction
NDP	– Neutron Depth Profiling
NI	– Neutron Imaging
NMR	– Nuclear Magnetic Resonance
OEMS	– Operando Electrochemical Mass Spectrometry (operando gas evolution analysis)
Raman	– Optical Raman spectroscopy
XAS	– X-Ray Absorption Spectroscopy
XPS	– X-Ray Photoelectron Spectroscopy
XRD	– X-Ray Diffraction
XR tomo	– X-Ray tomography (synchrotron in the present report)
XRS	– X-Ray Raman Scattering (synchrotron)
SAXS / WAXS	– Small Angle X-Ray Scattering / Wide Angle X-Ray Scattering
TEM – EELS	– Transmission Electron Microscopy – Electron Energy Loss Spectroscopy



5.2 LiTDI description and associated publications

LiTDI (lithium 4,5-dicyano-2-(trifluoromethyl)imidazolid), see Figure 32 for the chemical structure, is a salt used as an additive in the electrolyte that is believed to improve the SEI formation and stability as well as the global electrolyte stability upon ageing. Some capacity retention improvements have been reported in the literature on high Ni content active materials and in experiments conducted by WP6 partners. This explains why an electrolyte formulation containing LiTDI, with a composition tuned by WP6 partners according to their experiments on NMC, was investigated in D5.3 along with the standard BIG-MAP electrolyte, even though no improved cycling life was finally witnessed during the sample cycling by FZJ and CIDETEC. The LiTDI salt was synthesised and provided to FZJ by WUT (WP6).

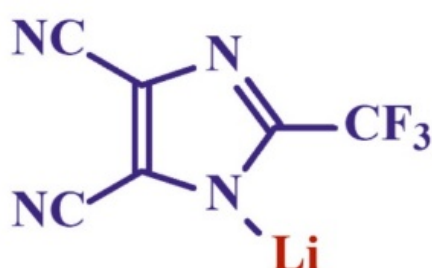


Figure 32. LiTDI chemical structure

Below are references on work reported in the literature related to the use of LiTDI in electrolytes for battery applications.

- [1] C. L. Berhaut, R. Dedryvère, L. Timperman, G. Schmidt, D. Lemordant, and M. Anouti, "A new solvent mixture for use of LiTDI as electrolyte salt in Li-ion batteries," *Electrochimica Acta*, vol. 305, pp. 534–546, May 2019, doi: [10.1016/j.electacta.2019.02.097](https://doi.org/10.1016/j.electacta.2019.02.097).
- [2] L. Niedzicki *et al.*, "New covalent salts of the 4+V class for Li batteries," *Journal of Power Sources*, vol. 196, no. 20, pp. 8696–8700, Oct. 2011, doi: [10.1016/j.jpowsour.2011.06.030](https://doi.org/10.1016/j.jpowsour.2011.06.030).
- [3] S. Paillet *et al.*, "Power capability of LiTDI-based electrolytes for lithium-ion batteries," *Journal of Power Sources*, vol. 294, pp. 507–515, Oct. 2015, doi: [10.1016/j.jpowsour.2015.06.073](https://doi.org/10.1016/j.jpowsour.2015.06.073).
- [4] S. Paillet *et al.*, "Determination of the electrochemical performance and stability of the lithium-salt, lithium 4,5-dicyano-2-(trifluoromethyl) imidazolid, with various anodes in Li-ion cells," *Journal of Power Sources*, vol. 299, pp. 309–314, Dec. 2015, doi: [10.1016/j.jpowsour.2015.08.102](https://doi.org/10.1016/j.jpowsour.2015.08.102).
- [5] R. Pan, Z. Cui, M. Yi, Q. Xie, and A. Manthiram, "Ethylene Carbonate-Free Electrolytes for Stable, Safer High-Nickel Lithium-Ion Batteries," *Advanced Energy Materials*, vol. 12, no. 19, p. 2103806, 2022, doi: [10.1002/aenm.202103806](https://doi.org/10.1002/aenm.202103806).
- [6] C. Xu *et al.*, "LiTDI: A Highly Efficient Additive for Electrolyte Stabilization in Lithium-Ion Batteries," *Chem. Mater.*, vol. 29, no. 5, pp. 2254–2263, Mar. 2017, doi: [10.1021/acs.chemmater.6b05247](https://doi.org/10.1021/acs.chemmater.6b05247).

5.3 Survey form used to gather D5.3 experimental result overview

Figure 33 is the form that was used to conduct the survey on D5.3 experimental results. This table (Excel spreadsheet) has been completed by every partner having performed experiments and has allowed the extraction of the meta-view discussed in section 3.3.

Partner name			
Experimental technique			
Experimental outputs:			
Are there differences between:			
with and without LiTDI cells	LNO	<i>yes/no/unsure/n.a.</i>	
	Gr	<i>yes/no/unsure/n.a.</i>	
Pristine and aged electrodes	LNO	<i>yes/no/unsure/n.a.</i>	
	Gr	<i>yes/no/unsure/n.a.</i>	
If there are differences, where are they?			
Material:		LNO	Gr
If between with and without LiTDI	Morphology	<i>yes/no/unsure/n.a.</i>	<i>yes/no/unsure/n.a.</i>
	Crystal structure	<i>yes/no/unsure/n.a.</i>	<i>yes/no/unsure/n.a.</i>
	Li distribution	<i>yes/no/unsure/n.a.</i>	<i>yes/no/unsure/n.a.</i>
	Phase transformation	<i>yes/no/unsure/n.a.</i>	<i>yes/no/unsure/n.a.</i>
	Reaction dynamic	<i>yes/no/unsure/n.a.</i>	<i>yes/no/unsure/n.a.</i>
	Homogeneity	<i>yes/no/unsure/n.a.</i>	<i>yes/no/unsure/n.a.</i>
	SEI and interfaces	<i>yes/no/unsure/n.a.</i>	<i>yes/no/unsure/n.a.</i>
	Electronic structure	<i>yes/no/unsure/n.a.</i>	<i>yes/no/unsure/n.a.</i>
	Other (please specify)	<i>yes/no/unsure/n.a.</i>	<i>yes/no/unsure/n.a.</i>
If between pristine and aged	Morphology	<i>yes/no/unsure/n.a.</i>	<i>yes/no/unsure/n.a.</i>
	Crystal structure	<i>yes/no/unsure/n.a.</i>	<i>yes/no/unsure/n.a.</i>
	Li distribution	<i>yes/no/unsure/n.a.</i>	<i>yes/no/unsure/n.a.</i>
	Phase transformation	<i>yes/no/unsure/n.a.</i>	<i>yes/no/unsure/n.a.</i>
	Reaction dynamic	<i>yes/no/unsure/n.a.</i>	<i>yes/no/unsure/n.a.</i>
	Homogeneity	<i>yes/no/unsure/n.a.</i>	<i>yes/no/unsure/n.a.</i>
	SEI and interfaces	<i>yes/no/unsure/n.a.</i>	<i>yes/no/unsure/n.a.</i>
	Electronic structure	<i>yes/no/unsure/n.a.</i>	<i>yes/no/unsure/n.a.</i>
	Other (please specify)	<i>yes/no/unsure/n.a.</i>	<i>yes/no/unsure/n.a.</i>
Is there a notable difference in manipulating the aged samples vs the pristine ones:	LNO	<i>yes/no/unsure/n.a.</i>	
	Gr	<i>yes/no/unsure/n.a.</i>	

If you have several experimental techniques please copy/paste this table ensemble and fill one per experimental technique.

For each item in the "experimental outputs" section please choose and answer between yes/no/unsure/n.a.
 n.a. = non applicable
 unsure = not clear (yet)
 yes = clear differences
 no = no noticeable differences at all

We do not need much more for the D5.3 summary reporting, in addition to the experimental reports. If you would like to add something, feel free to use the "additional information" text box below the table.

Additional information: *(optional)*

Figure 33. Form used to conduct the survey on the overview of the experimental results from D5.3

5.4 Additional plots for the D5.3 scientific outcomes

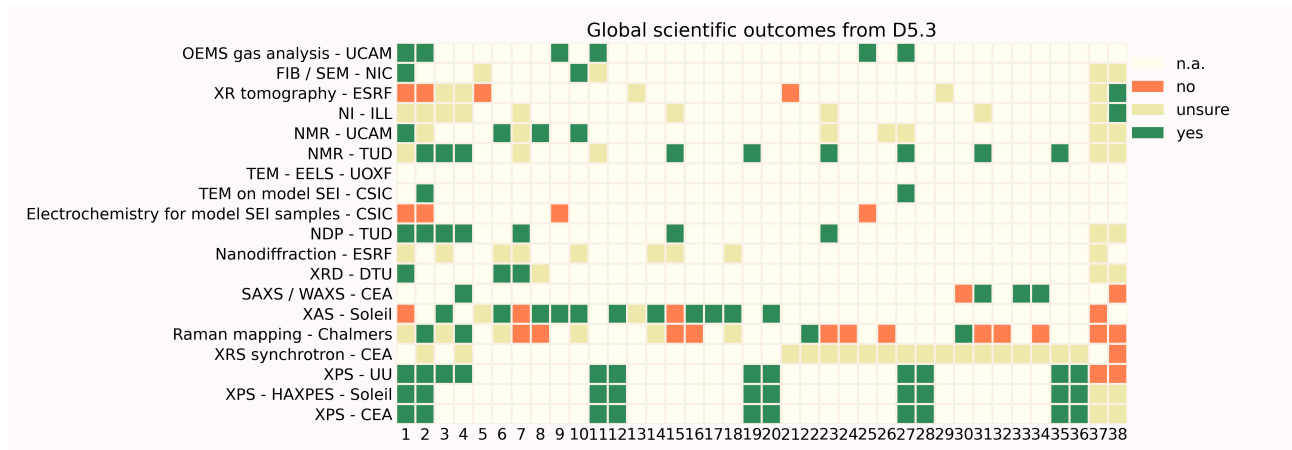


Figure 34. Global overview of the scientific outcomes from D5.3

Column label legend:

- 1 - Difference between with and without LiTDI in LNO electrodes
- 2 - Difference between with and without LiTDI in Gr electrodes
- 3 - Difference between pristine and aged electrodes in LNO electrodes
- 4 - Difference between pristine and aged electrodes in Gr electrodes
- 5 - LiTDI induces morphology changes in LNO electrodes
- 6 - LiTDI induces crystal structure changes in LNO electrodes
- 7 - LiTDI induces Li distribution changes in LNO electrodes
- 8 - LiTDI induces phase transformation changes in LNO electrodes
- 9 - LiTDI induces reaction dynamic changes in LNO electrodes
- 10 - LiTDI induces homogeneity changes in LNO electrodes
- 11 - LiTDI induces SEI/interfaces changes in LNO electrodes
- 12 - LiTDI induces electronic structure changes in LNO electrodes
- 13 - Ageing induces morphology changes in LNO electrodes
- 14 - Ageing induces crystal structure changes in LNO electrodes
- 15 - Ageing induces Li distribution changes in LNO electrodes
- 16 - Ageing induces phase transformation changes in LNO electrodes
- 17 - Ageing induces reaction dynamic changes in LNO electrodes
- 18 - Ageing induces homogeneity changes in LNO electrodes
- 19 - Ageing induces SEI/interfaces changes in LNO electrodes
- 20 - Ageing induces electronic structure changes in LNO electrodes
- 21 - LiTDI induces morphology changes in Gr electrodes
- 22 - LiTDI induces crystal structure changes in Gr electrodes
- 23 - LiTDI induces Li distribution changes in Gr electrodes
- 24 - LiTDI induces phase transformation changes in Gr electrodes
- 25 - LiTDI induces reaction dynamic changes in Gr electrodes
- 26 - LiTDI induces homogeneity changes in Gr electrodes
- 27 - LiTDI induces SEI/interfaces changes in Gr electrodes
- 28 - LiTDI induces electronic structure changes in Gr electrodes
- 29 - Ageing induces morphology changes in Gr electrodes
- 30 - Ageing induces crystal structure changes in Gr electrodes
- 31 - Ageing induces Li distribution changes in Gr electrodes
- 32 - Ageing induces phase transformation changes in Gr electrodes
- 33 - Ageing induces reaction dynamic changes in Gr electrodes
- 34 - Ageing induces homogeneity changes in Gr electrodes
- 35 - Ageing induces SEI/interfaces changes in Gr electrodes
- 36 - Ageing induces electronic structure changes in Gr electrodes
- 37 - Ageing induces changes in manipulating LNO electrodes
- 38 - Ageing induces changes in manipulating Gr electrodes

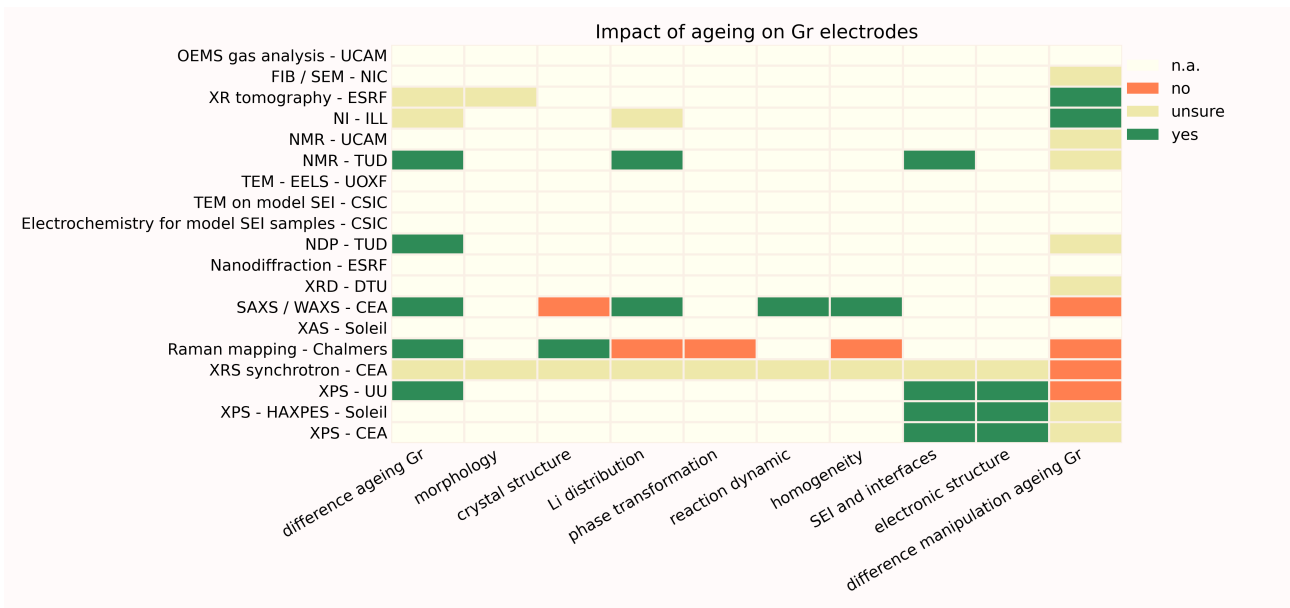


Figure 35. Scientific outcomes from D5.3 related to the effect of ageing on graphite electrodes

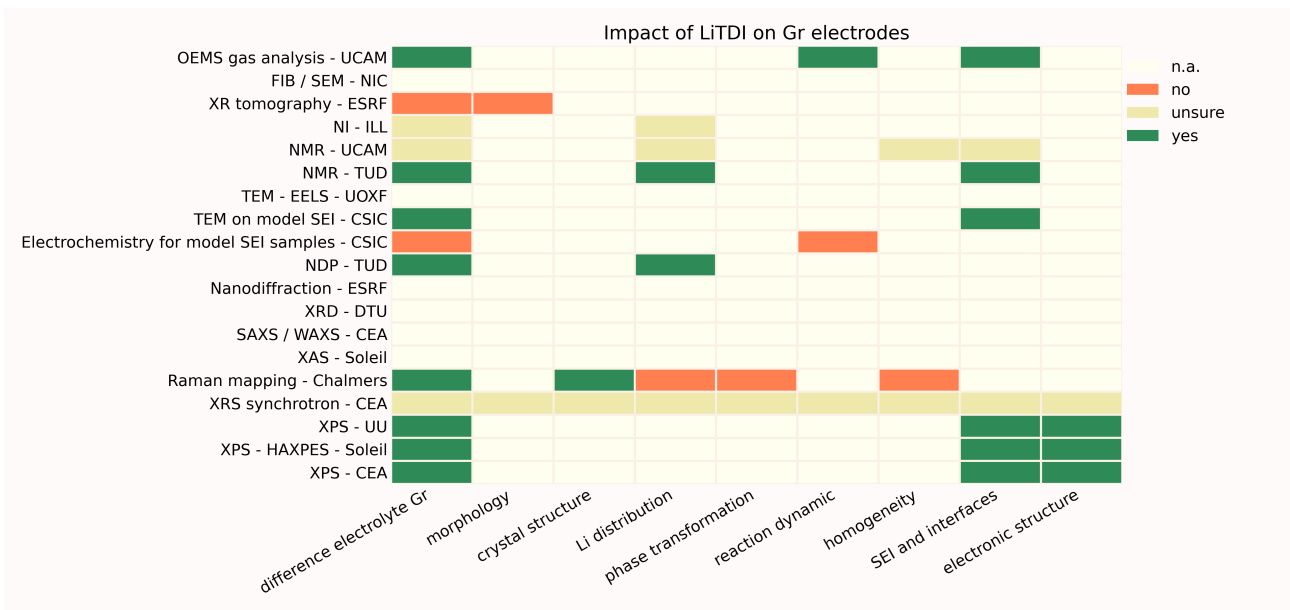


Figure 36. Scientific outcomes from D5.3 related to the effect of LiTDI on graphite electrodes

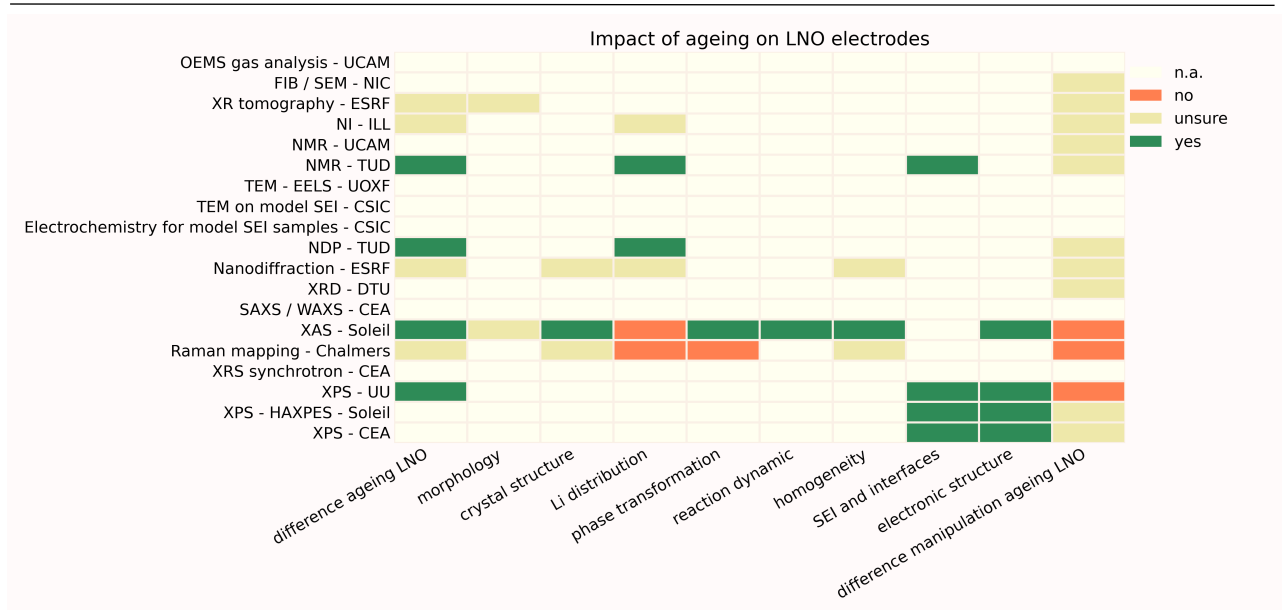


Figure 37. Scientific outcomes from D5.3 related to the effect of ageing on LNO electrodes

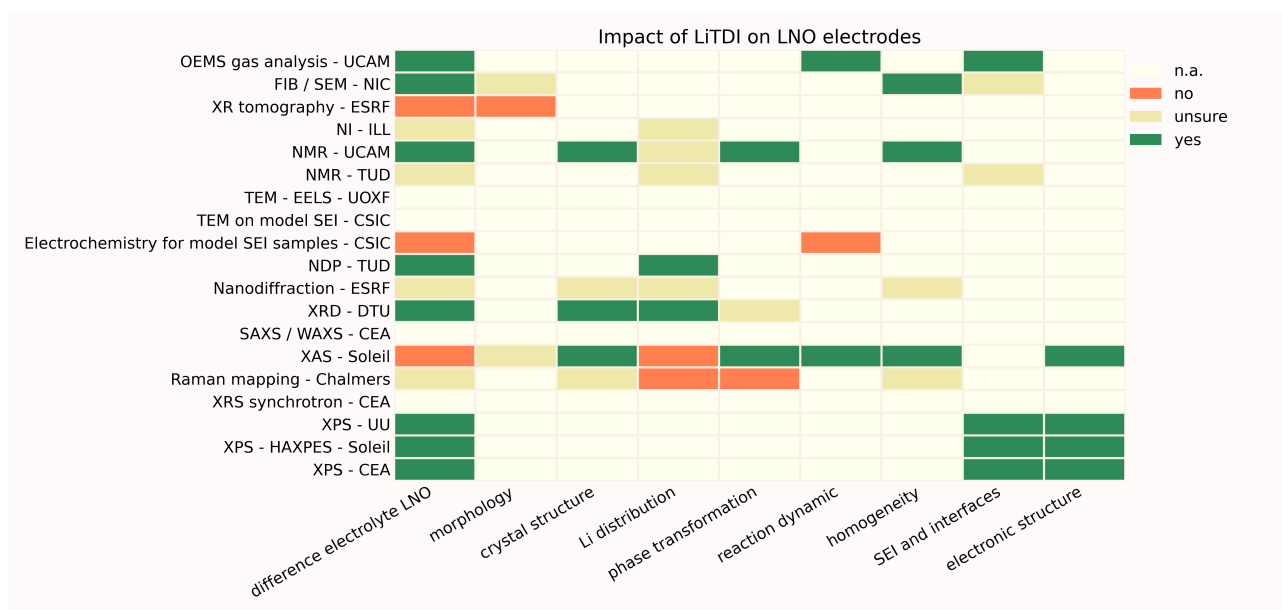
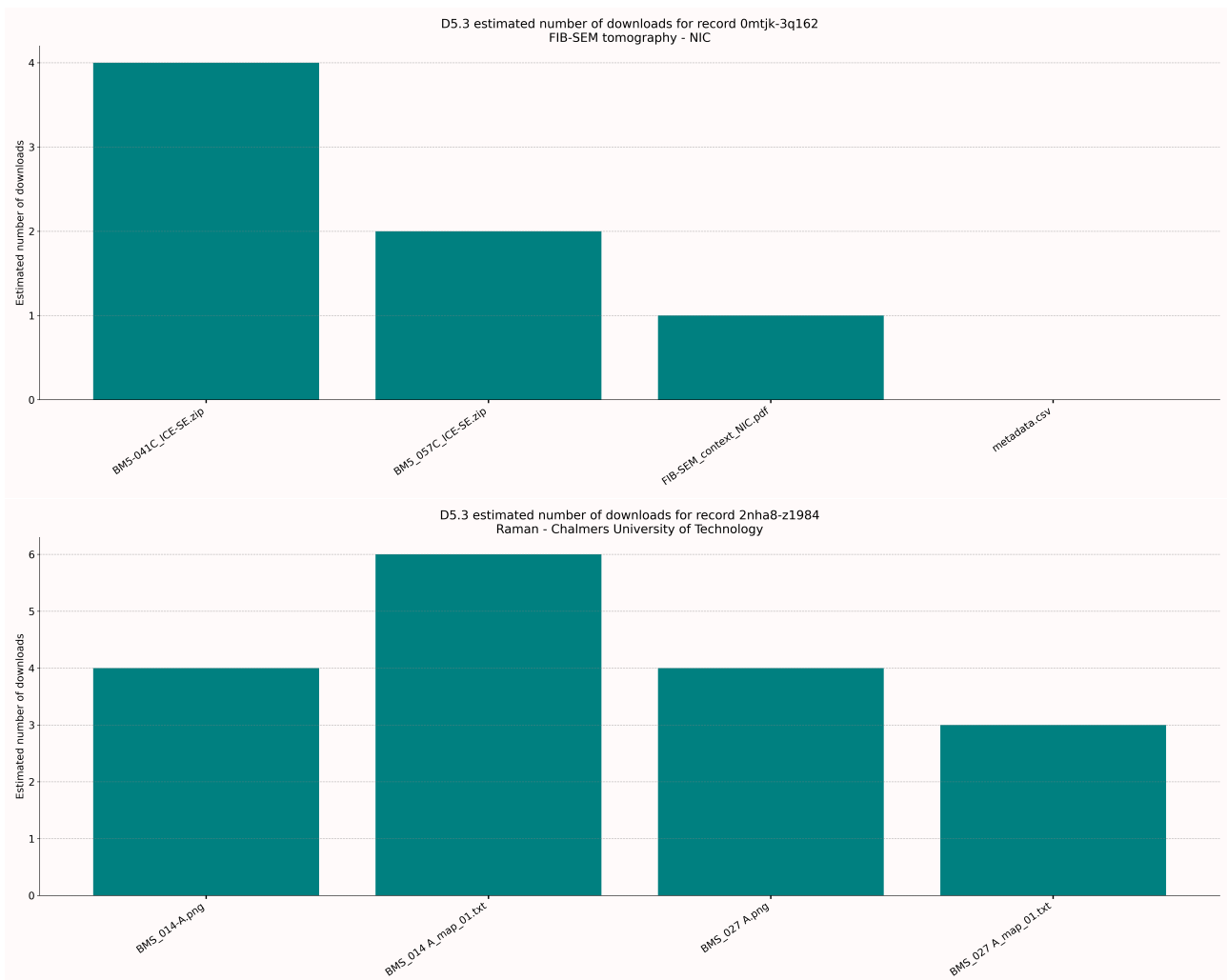
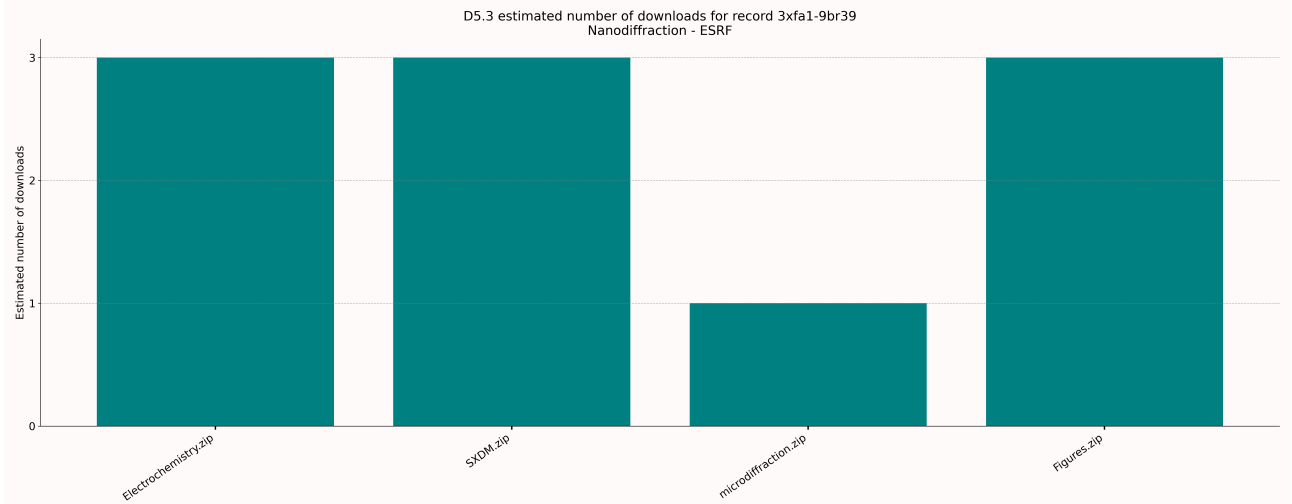
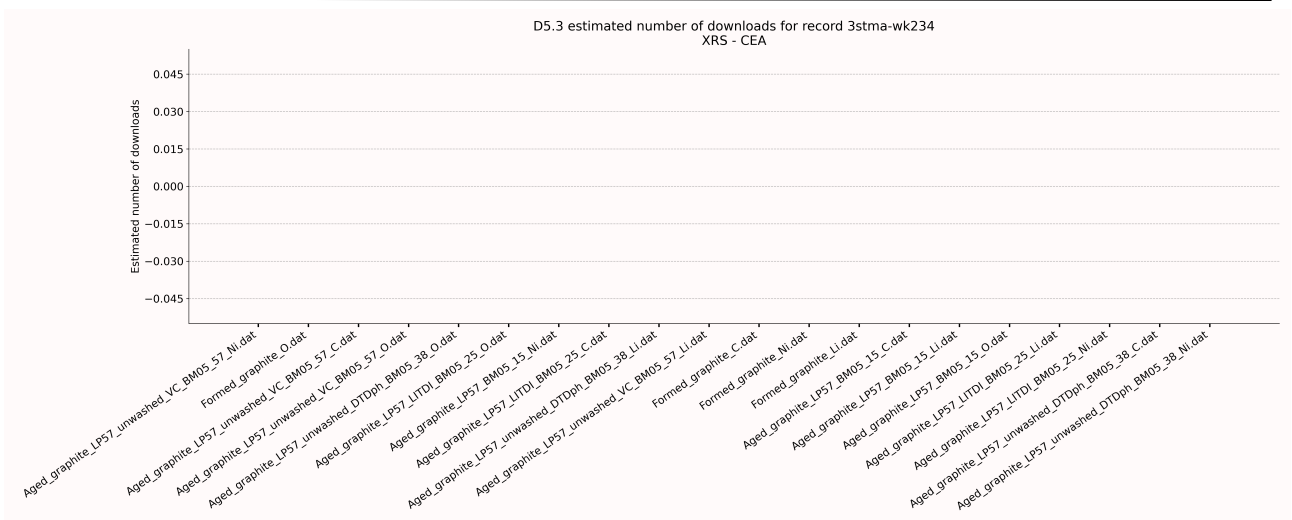


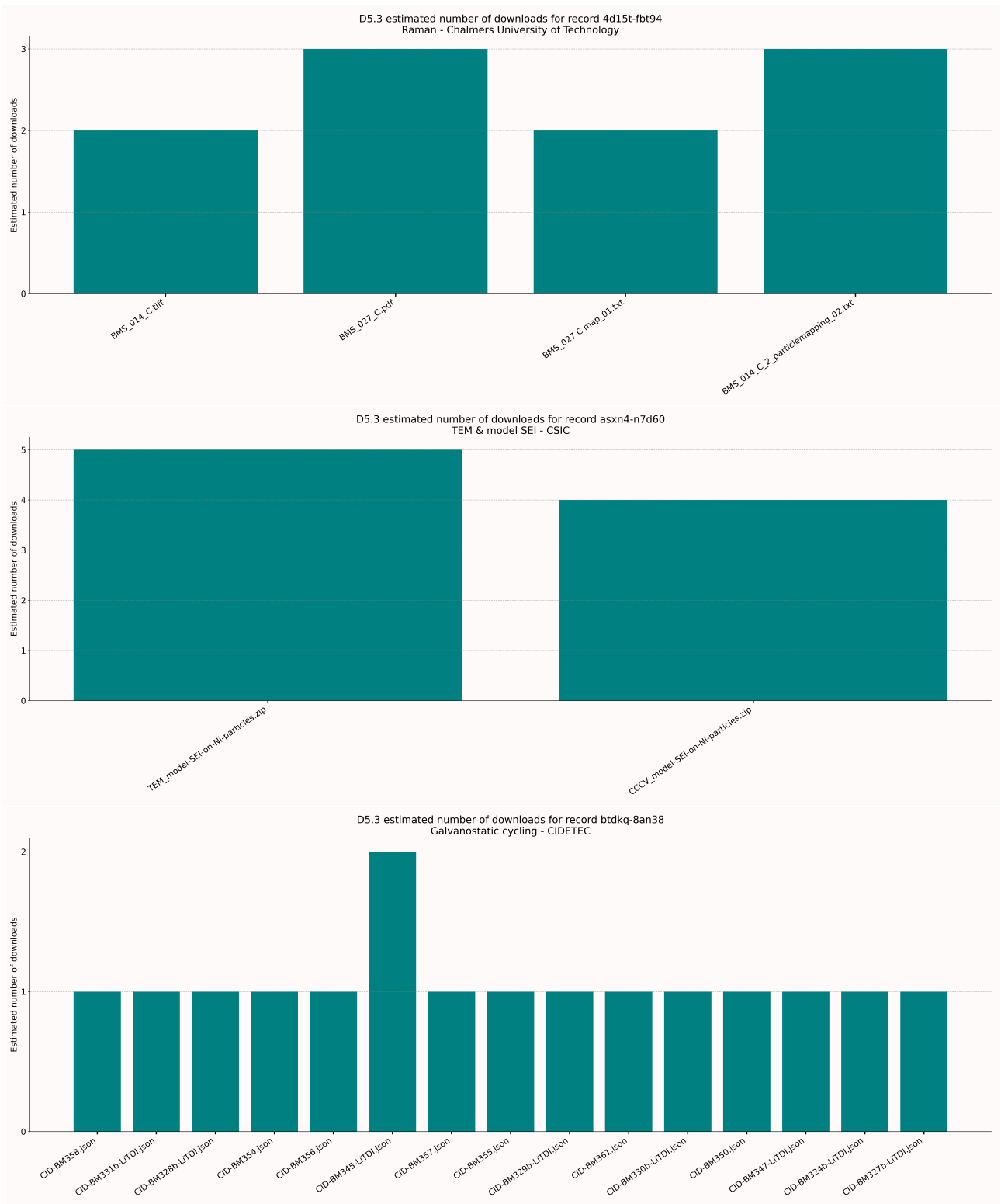
Figure 38. Scientific outcomes from D5.3 related to the effect of LiTDI on LNO electrodes

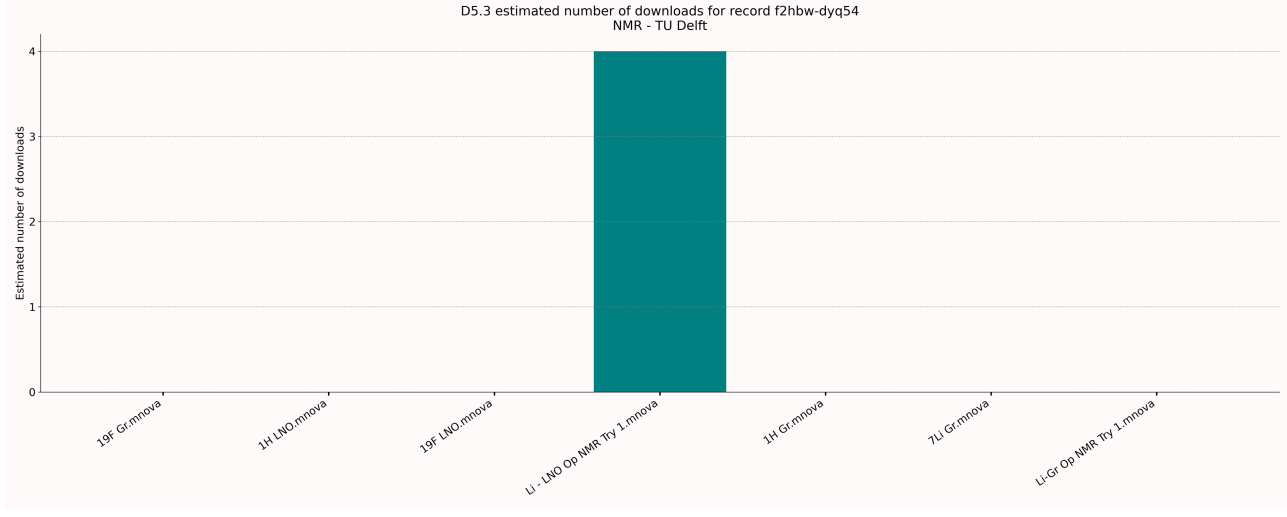
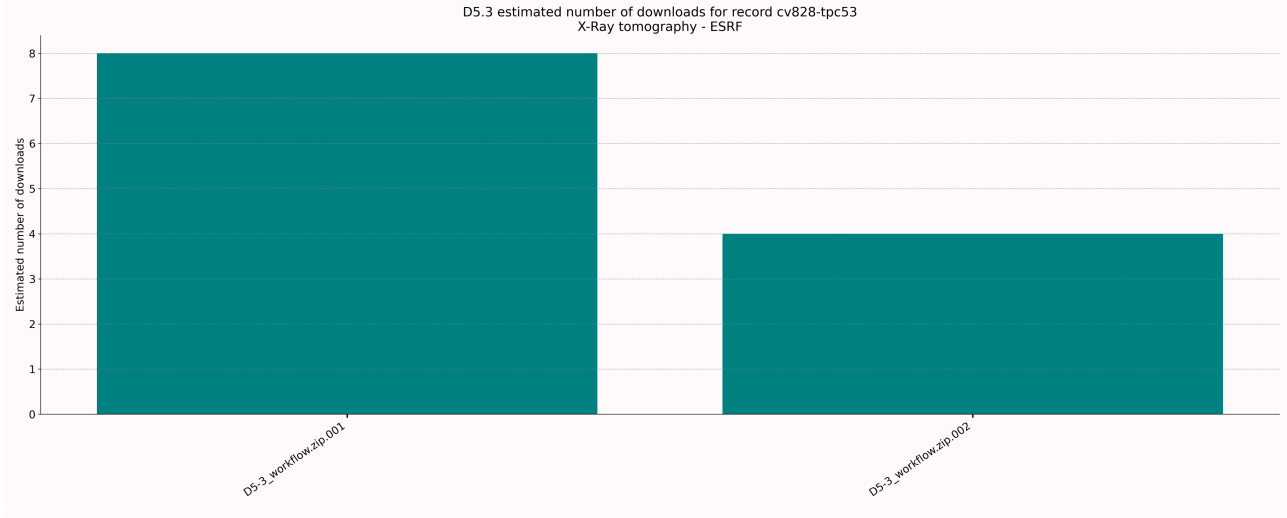
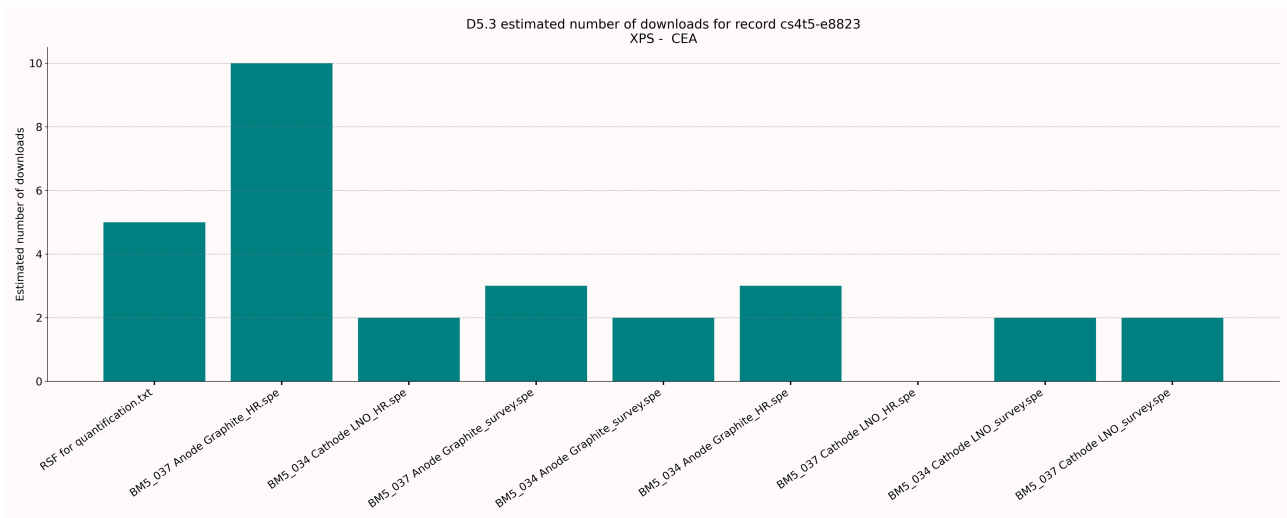
5.5 Additional information on the BIG-MAP Archive usage

Below are reported the download statistics detailed over each file per record linked to the D5.3 experiments. The record ID (constituting the unique record url when added to the root link <https://archive.big-map.eu/records>, e.g. <https://archive.big-map.eu/records/ggvxb-z1a82>), along with the partner and experimental technique, is reported in the title of each plot in the upper part and the file names are mentioned in the abscissa. Such statistics can help detailing which subsets are more popular from the datasets in each record. This can be an interesting information when building subsequent workflows around similar questions and / or using some of these techniques. It is worth noticing that some records are showing no, or very few, recorded dataset downloads (graph 3, 11 and 12). These are very recent as per the update date for the data in the current annex (cf. Figure 24) which can explain this state. Statistics were last updated on 07/08/2023.









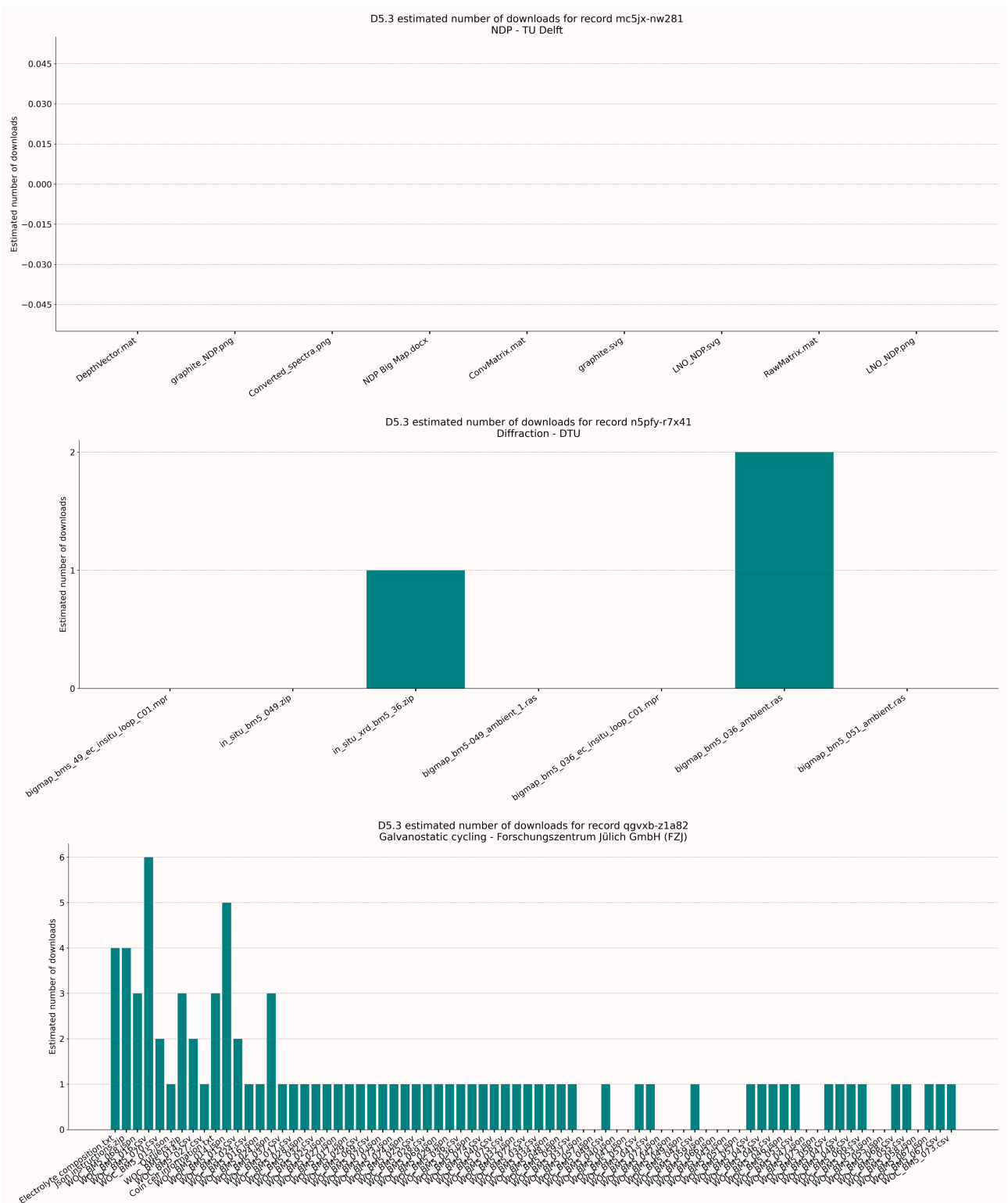


Figure 39. Estimated number of downloads detailed per file in records linked to D5.3 and shared on the BIG-MAP Archive